12-2007

Thermodynamic Characterization of Aminoglycoside-3'-Phosphotransferase IIIa

Can Özen
University of Tennessee - Knoxville

To the Graduate Council:

I am submitting herewith a dissertation written by Can Özen entitled "Thermodynamic Characterization of Aminoglycoside-3'-Phosphotransferase IIIa." I have examined the final electronic copy of this dissertation for form and content and recommend that it be accepted in partial fulfillment of the requirements for the degree of Doctor of Philosophy, with a major in Life Sciences.

Engin H. Serpersu, Major Professor

We have read this dissertation and recommend its acceptance:

Michael Best, Hong Guo, Nitin Jain

Accepted for the Council:

Carolyn R. Hodges

Vice Provost and Dean of the Graduate School

(Original signatures are on file with official student records.)

To the Graduate Council:

I am submitting herewith a dissertation written by Can Özen entitled "Thermodynamic Characterization of Aminoglycoside-3′-Phosphotransferase IIIa." I have examined the final electronic copy of this dissertation for form and content and recommend that it be accepted in partial fulfillment of the requirements for the degree of Doctor of Philosophy, with a major in Life Sciences.

_____
Engin H. Serpersu, Major Professor

We have read this dissertation
and recommend its acceptance:

Michael Best_____

Hong Guo_____

Nitin Jain_____

Accepted for the Council:

_____
Carolyn R. Hodges, Vice Provost and
Dean of the Graduate School

(Original signatures are on file with official student records.)

Thermodynamic Characterization of Aminoglycoside-3′-Phosphotransferase IIIa

A Dissertation Presented for
the Doctor of Philosophy
Degree
The University of Tennessee, Knoxville

Can Özen
December 2007

Acknowledgements

I want to thank Dr. Engin Serpersu for his guidance and support.

I want to acknowledge my committee members, Drs. Nitin Jain, Hong Guo, and Michael Best for their helpful suggestions and input.

I want to thank Drs. Elizabeth Howell, Elias Fernandez and Chris Dealwis for their valuable comments.

I am grateful to all previous and present members of the Serpersu Lab who I've worked with for their help in my studies.

I want to thank my wife Aysu Özen, my mother and father, Gökçen and Mehmet Özen, and my brother, Cem Özen for being there for me. Your love and support kept me going.

Abstract

Aminoglycoside-3′-Phosphotransferase IIIa is a widespread, promiscuous member of the phosphotransferase family of aminoglycoside modifying enzymes. This study provides results of combined calorimetry/NMR experiments to characterize and dissect the global thermodynamic properties of aminoglycoside–APH(3′)-IIIa complexes. Aminoglycoside binding to APH(3′)-IIIa is enthalpically driven with strong entropic penalty. 2′- and 6′-amino groups have significant contributions to the observed binding parameters. Formation of APH(3′)-IIIa complexes with substrate aminoglycosides shows a complex dependence on pH and is linked to protonation and deprotonation of both ligand and enzyme groups. We report pK_a upshifts of ~1 unit for N2′ and N2‴ groups of enzyme-bound neomycin B while the pK_a of N6′ changes by 0.3 unit and N6‴ experiences no shift. Isotopic solvent and heat capacity change studies strongly suggest differential effects and reorganization of solvent in kanamycin and neomycin class complexes of the enzyme. We also determined unusually high binding ΔCp values in the range of -0.7 to -3.8 kcal/mol·deg which were not explained by changes in the solvent accessible surface area. A break at 30°C was observed in the ΔCp plot and temperature-dependent backbone amide proton chemical shifts of four residues surrounding the binding site of kanamycin-APH(3′)-IIIa complex. These results may indicate specific solvent reorganization sites away from the binding site of the enzyme.

Table of Contents

List of Tables

Table **Page**

List of Figures

Figure **Page**

PART IV

APPENDIX

PART I. INTRODUCTION

Aminoglycoside Antibiotics

Aminoglycosides are highly potent, broad spectrum antibiotics. They can be used in synergy with other antibiotics and have predictable pharmacokinetics (*1-3*). The first aminoglycoside, streptomycin, was discovered in 1943 and has been very effective against highly serious infectious diseases of the time such as tuberculosis and the plague (*4*). Since then, various natural and synthetic aminoglycosides have been discovered or synthesized. Although clinical application of aminoglycosides is limited due to their side effects (renal and auditory toxicity) (*5*) and microbial resistance associated with widespread and misuse through decades, they are still in use, especially against nosocomial infections such as *staphylococci* and *enterococci*.

The cellular target for aminoglycosides is the 16S rRNA section of the 30S ribosomal subunit (*3, 6, 7*). When they bind to their RNA target, aminoglycosides interfere with translational fidelity (misreading and inhibition of translocation) and cause premature termination of protein biosynthesis. Loss of function in membrane associated proteins increases cellular intake of aminoglycosides and eventually causes cell death.

Aminoglycosides are structurally diverse hydrophilic sugar molecules carrying several amino and hydroxyl functional groups. At physiological pH, amino groups are partially protonated and make these molecules polycationic in nature. Aminoglycosides are carbohydrate molecules composed of two or more amino sugars linked by glycosidic bonds to an aminocyclitol ring, typically a 2-deoxystreptamine (2-DOS). 2-DOS aminoglycosides are classified as 4,5-disubstituted (neomycin) and 4,6-disubstituted (kanamycin) based on the substitution positions of the 2-DOS ring (Figure 1).

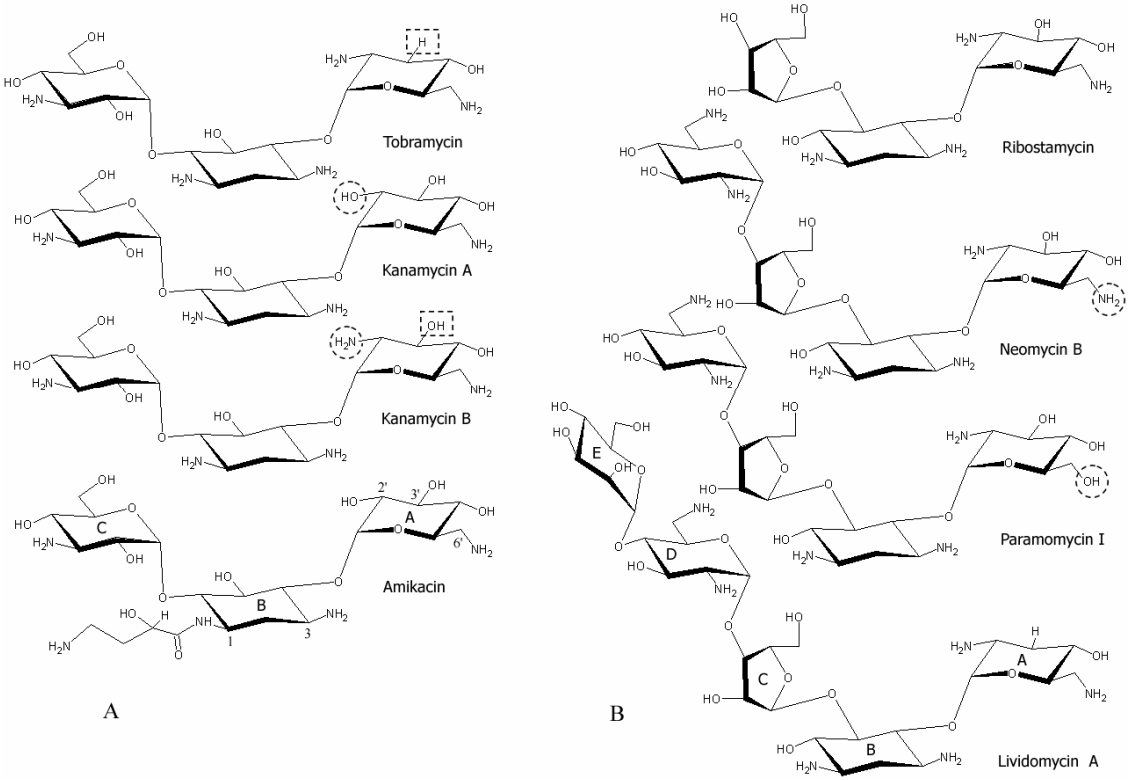

Figure 1. Structures of aminoglycosides containing a (A) 4,6-disubstituted or (B) 4,5-disubsituted 2-DOS ring. Single functional group differences between structurally similar aminoglycosides are indicated with dotted circles marking the 2′- and 6′-positions in (A) and (B), respectively. Dotted squares in (A) show the 3′-position. Rings A, B, C, D, and E are also named as primed (′), unprimed, double primed (″), triple primed (‴), and quadruple primed (⁗) respectively. The numbering of carbon atom positions is shown on the amikacin structure.

Aminoglycoside Modifying Enzymes

Bacterial cells use various defensive measures against aminoglycosides such as efflux pumps, decreased intake and ribosomal structure modification (*8*). However, the most common bacterial resistance mechanism is enzymatic modification by Aminoglycoside Modifying Enzymes (AMEs) (*7, 9*). Aminoglycoside molecules covalently modified by these enzymes rendered ineffective due to poor cellular uptake and ribosome binding.

There are more than 50 AME genes have been identified in plasmids, transposons and chromosomes of bacteria (*9*). There may be several genetic variants of the same enzyme. For example, AAC(6′)-I enzyme has 26 variants (*10*). On the basis of modification reaction, the enzymes encoded by these genes are collected under three groups; aminoglycoside nucleotidyltransferases (ANTs), phosphotransferases (APHs) and acetyltransferases (AACs). Sequence similarity is low between AME families.

AMEs are promiscuous with respect to the aminoglycoside substrates, and the same enzyme can modify several structurally different aminoglycoside antibiotics. Furthermore, any given antibiotic can be modified by many different enzymes at the same or different site(s) on the antibiotic. Figure 2 shows three AMEs studied in our laboratory and their target modification sites on a common substrate; kanamycin A.

Largest group of the AMEs is the acetyltransferase family. These enzymes carry out acetyl-coenzyme A dependent N-acetylation of the target amino groups of substrate aminoglycosides. There are four sub-classes which can modify aminoglycosides at 1-, 3-, 6′- and 2′- amino positions (*9*). Enzymes grouped under AAC family belong to the

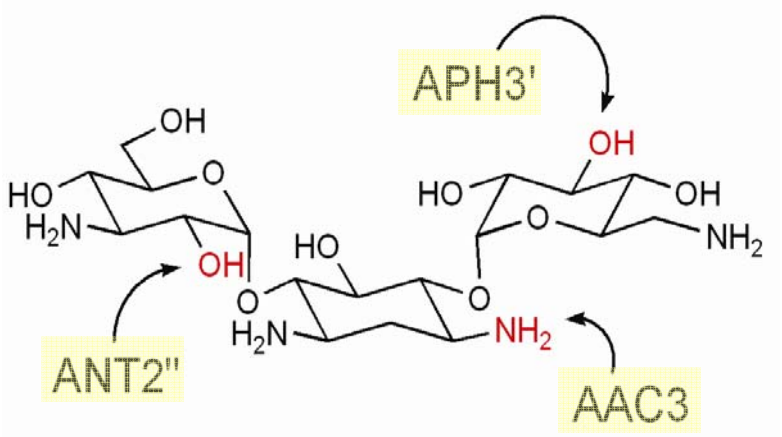

Figure 2. Aminoglycoside modifying enzymes studied in our laboratory. Target modification sites for each enzyme is labeled red and indicated with an arrow.

GCN5-related N-Acetyltransferases (GNAT) superfamily which also includes yeast and human histone acetyltransferases. ANT family, the smallest of the three groups with less than ten members, is typically related to resistance by Gram-negative bacteria (*11*). ATP is the donor group in adenylation reaction. The most frequent targets for modification are hydroxyl groups at 4′ and 2″. The aminoglycoside phosphotransferase family (APHs) is the second largest group of aminoglycoside modifying enzymes, which contains eight main types; APH(3′)-I through APH(3′)-VIII (*9*). APH(3′)-IIIa is the most widespread resistance associated member of this group. It is commonly expressed in *Enterococci, Streptococci* and *Staphylococci* strains. Like ANTs, APH enzymes also use ATP as the coenzyme. Extensive sequence identity (20-40%) is shared between the family members.

3D structure of several AMEs from three families have been resolved in recent years. Comparison to functionally related eukaryotic protein structures reveals remarkable similarities. For example, there is a high degree of structural similarity

between APH(3′) sub family and prokaryotic and eukaryotic protein kinases. Typical two-domain structure of kinases is also observed in APH enzymes. N-terminal and C-terminal domains of known APH(3′) structures and cAMP kinase superimpose with very small RMS values although they don't share a sequence similarity. Some eukaryotic protein kinase (EPK) inhibitors can inhibit APH(3')-IIIa and AAC(6')-APH(2"). Additional studies following this observation indicates that APH(3')-IIIa and AAC(6')-APH(2") can phosphorylate some EPK peptide substrates at serine residues (*12*).

Aminoglycoside Phosphotransferase(3′)-IIIa

APH(3′)-IIIa (NCBI protein databank: P00554, Expasy: P00554) is the most promiscuous member of APH 3′-subfamily (*13*). APH(3′)-IIIa gene has been cloned from pJH1 R-plasmid isolated from an *Enterococcus faecalis* clinical isolate. It shows significant homology to other members of APH(3′) subfamily (*9, 14*). Protein sequence is composed of 264 amino acids with a molecular weight of 31 kDa. Under non-reducing conditions, APH(3′)-IIIa forms dimer through two sulfide bridges between residues Cys19 and Cys156.

APH(3′)-IIIa can phosphorylate at least ten different aminoglycoside antibiotics. The modification reaction is ATP-dependent O-phosphorylation of 3′ and/or 5″ (in the case of neomycin class) hydroxyl group. Mg^{++} is an essential ion required for activity through the coordination of ATP in the active site. Specificity constants (k_{cat}/K_m) is typically on the order of 10^5 $M^{-1}s^{-1}$. Steady state kinetics studies indicate a special case of ordered Bi-Bi kinetic mechanism for APH(3′)-IIIa called Theorell–Chance in which ATP

binds first with rapid equilibrium followed by aminoglycoside binding, release of phosphorylated aminoglycoside and rate-limiting step of ADP release (*15-19*) (Figure 3).

A dissociative catalytic mechanism (Figure 4) was proposed for the phosphoryl transfer reaction catalyzed by the enzyme where nucleophilic attack of 3′-hydroxyl oxygen of the aminoglycoside on the γ-phosphate of ATP takes place after the bond between leaving phosphate group and β-phosphate is broken. According to the proposed model, a metaphosphate-like transition state which is stabilized by Mg^{+2} ion and Asp208 forms. Residues Met26 and Ser27 also play critical roles in catalysis by interacting with β- and γ-phosphate groups of ATP respectively. Initial aminoglycoside deprotonation was found to be not essential for the phosphate transfer (*20*).

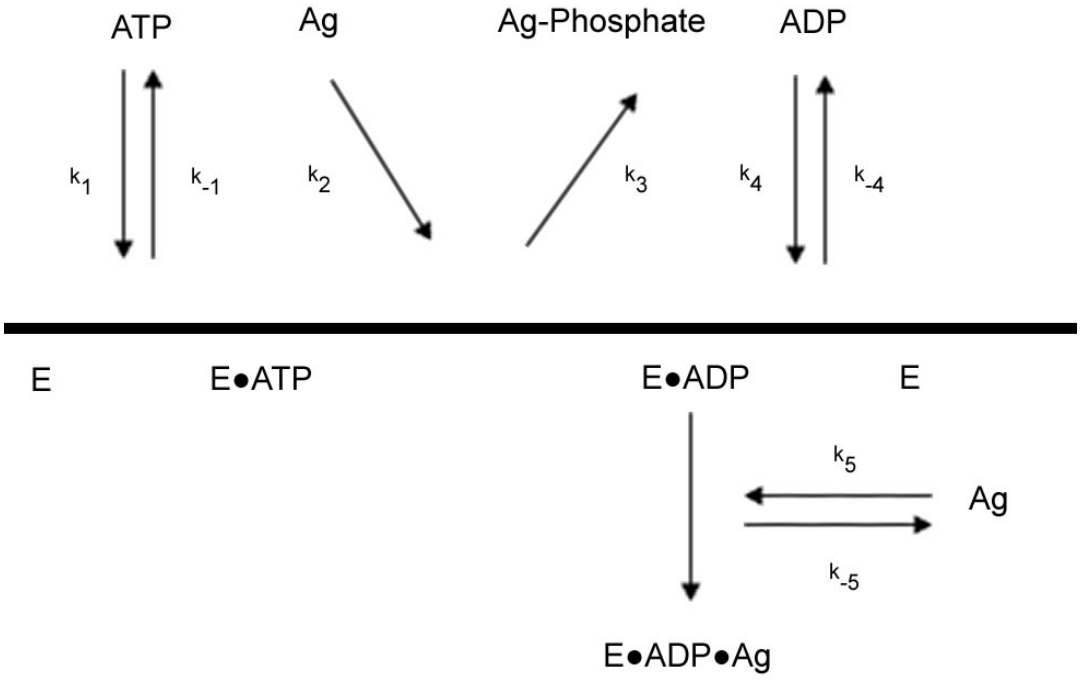

Figure 3. Theorell-Chance kinetic mechanism of APH(3′)-IIIa. ATP binding is followed

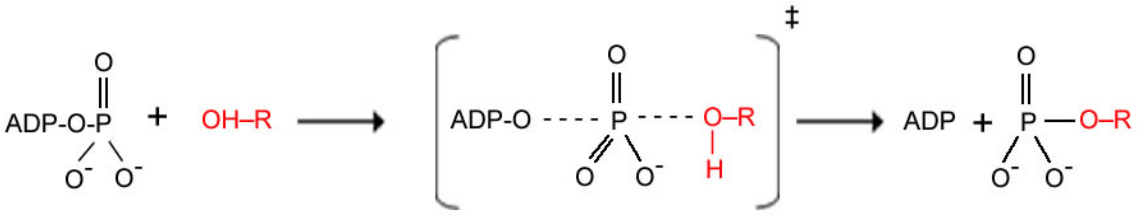

Figure 4. The catalytic mechanism of APH(3′)-IIIa. 3′-OH position of the substrate aminoglycoside is labeled red. The metaphosphate-like transition state is indicated in the middle.

by aminoglycoside (Ag) binding. Following group transfer, phosphorylated aminoglycoside (Ag-Phosphate) is released. ADP dissociation is the last and rate-limiting step.

Several APH(3′)-IIIa crystal structures have become available in recent years. Structure of the holo-enzyme (ADP and AMP-PNP bound) was provided by Hon et. al. (*21*) followed by the release of the apo-form structure by Berk et. al. (*22*). The first aminoglycoside substrate bound structures (kanamycin A and neomycin B) of APH(3′)-IIIa were resolved by Fong et. al. in 2002 (Figure 5) (*13*). Our laboratory studied enzyme bound conformations of amikacin and butirosin A using APH(3′)-IIIa (23-*25*).

Part I of this thesis presents the first published work on general thermodynamic characterization of aminoglycoside-APH(3′)-IIIa interactions. In Part II, we report, again for the first time, pK_a values of an enzyme bound aminoglycoside and use this information to dissect the calorimetrically-derived global proton-linkage data. The following chapter focuses on solvent effects and heat capacity change of aminoglycoside-APH(3′)-IIIa complexes using a combined calorimetry/NMR approach.

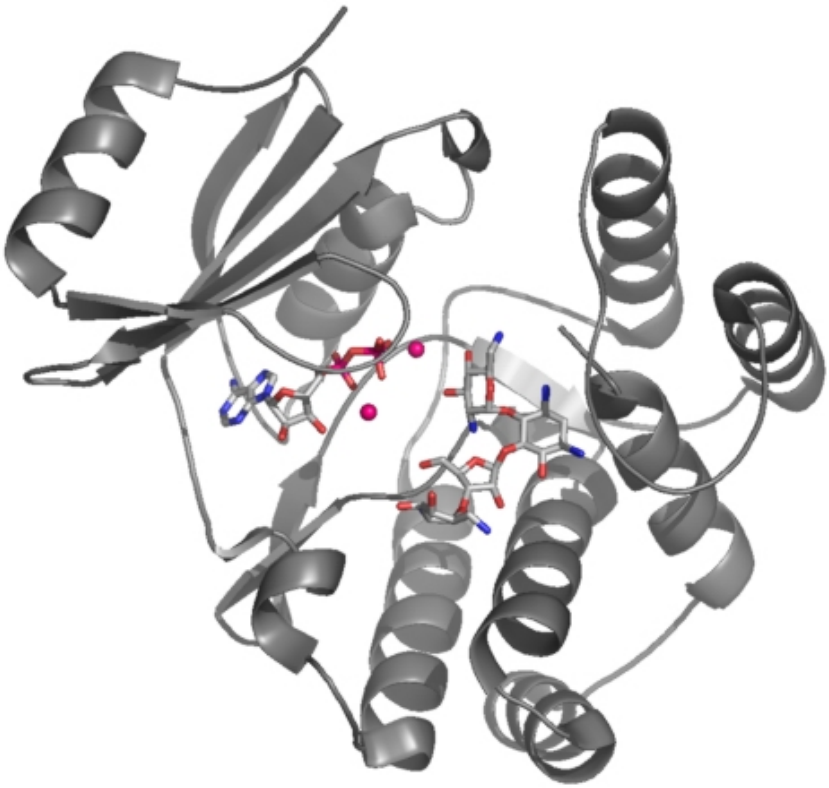

Figure 5. Structure of the ternary neomycin B-ADP-APH(3′)-IIIa complex. Mg^{++} ions are shown as pink spheres.

List of References

References

(1) Davies, J. E. (1991) in *Antibiotics in Laboratory Medicine* (Lorian, V., Ed.) pp 691-713, Williams and Wilkins, Baltimore.

(2) Mingeot-Leclercq, M. P., Glupczynski, Y., and Tulkens, P. M. (1999) Aminoglycosides: activity and resistance. *Antimicrob. Agents Chemother. 43*, 727-37.

(3) Umezawa, H. (1974) Biochemical mechanism of resistance to aminoglycosidic antibiotics. *Adv. Carbohydr. Chem. Biochem. 30*, 183-225.

(4) Schatz, A., Bugie, E., Waksman, S.A. (1944). Streptomycin, a substance exhibiting antibiotic activity against gram-positive and gram-negative bacteria. *Proc. Soc. Exp. Biol. Med.* 55, 66-69.

(5) Forge, A., and Schacht, J. (2000) Aminoglycoside antibiotics. *Audiol. Neurootol. 5*, 3-22.

(6) Moazed, D., and Noller, H. F. (1987) Interaction of antibiotics with functional sites in 16S ribosomal RNA. *Nature 327*, 389-94.

(7) Davies, J. (1994) Inactivation of antibiotics and the dissemination of resistance genes. *Science 264*, 375-82.

(8) Benveniste, R., and Davies, J. (1973) Mechanisms of antibiotic resistance in bacteria. *Annu. Rev. Biochem. 42*, 471-506.

(9) Shaw, K. J., Rather, P. N., Hare, R. S., and Miller, G. H. (1993) Molecular genetics of aminoglycoside resistance genes and familial relationships of the aminoglycoside-modifying enzymes. *Microbiol. Rev. 57*, 138-63.

(10) Smith, C. A., and Baker, E. N. (2002) Aminoglycoside antibiotic resistance by enzymatic deactivation. *Curr. Drug Targets Infect. Disord. 2*, 143-60.

(11) Miller G.H., Sabatelli F.J., Hare R.S., Glupczynski Y., Mackey P., Shlaes D., Shimizu K., and Shaw K.J. (1997). The most frequent aminoglycoside resistance mechanisms--changes with time and geographic area: a reflection of aminoglycoside usage patterns? Aminoglycoside Resistance Study Groups. *Clin. Infect. Dis.* Jan;24 Suppl 1:S46-62.

(12) Daigle, D. M., McKay G. A., Thompson, P. R., and Wright, G. D. (1999) Aminoglycoside antibiotic phosphotransferases are also serine protein kinases. *Chem. Biol. 6*, 11-18.

(13) Fong, D. H., and Berghuis, A. M. (2002) Substrate promiscuity of an aminoglycoside antibiotic resistance enzyme via target mimicry. *Embo J 21*, 2323-31.

(14) Trieu-Cuot P., and Courvalin P. (1983). Nucleotide sequence of the Streptococcus faecalis plasmid gene encoding the 3'5"-aminoglycoside phosphotransferase type III. *Gene.* Sep;23(3):331-41.

(15) McKay, G. A., and Wright, G. D. (1996) Catalytic mechanism of enterococcal kanamycin kinase (APH(3')-IIIa): viscosity, thio, and solvent isotope effects support a Theorell-Chance mechanism. *Biochemistry 35*, 8680-5.

(16) McKay, G. A., Robinson, R. A., Lane, W. S., and Wright, G. D. (1994) Active-site labeling of an aminoglycoside antibiotic phosphotransferase (APH(3')-IIIa). *Biochemistry 33*, 14115-20.

(17) McKay, G. A., Roestamadji, J., Mobashery, S., and Wright, G. D. (1996) Recognition of aminoglycoside antibiotics by enterococcal-staphylococcal aminoglycoside 3'-phosphotransferase type IIIa: role of substrate amino groups. *Antimicrob. Agents Chemother. 40*, 2648-50.

(18) McKay, G. A., Thompson, P. R., and Wright, G. D. (1994) Broad spectrum aminoglycoside phosphotransferase type III from Enterococcus: overexpression, purification, and substrate specificity. *Biochemistry 33*, 6936-44.

(19) McKay, G. A., and Wright, G. D. (1995) Kinetic mechanism of aminoglycoside phosphotransferase type IIIa. Evidence for a Theorell-Chance mechanism. *J. Biol. Chem. 270*, 24686-92.

(20) Boehr, D. D., Thompson, P. R., and Wright, G. D. (2001) Molecular mechanism of aminoglycoside antibiotic kinase APH(3')-IIIa: roles of conserved active site residues. *J. Biol. Chem.* 276, 23929-36.

(21) Hon, W. C., McKay, G. A., Thompson, P. R., Sweet, R. M., Yang, D. S., Wright, G. D., and Berghuis, A. M. (1997) Structure of an enzyme required for aminoglycoside antibiotic resistance reveals homology to eukaryotic protein kinases. *Cell 89*, 887-95.

(22) Burk, D. L., Hon, W. C., Leung, A. K., and Berghuis, A. M. (2001) Structural analyses of nucleotide binding to an aminoglycoside phosphotransferase. *Biochemistry 40*, 8756-64.

(23) Cox, J. R. (1997) Biologically Important Conformations of Aminoglycoside Antibiotics Bound to an Aminoglycoside 3'-Phosphotransferase as Determined by Transferred Nuclear Overhauser Effect Spectroscopy. *Biochemistry 36*, 2353-59.

(24) Cox, J. R., McKay, G. A., Wright, G. D., and Serpersu, E. H. (1996) Arrangement of substrates at the active site of an aminoglycoside antibiotic 3'-phosphotransferase as determined by NMR. *Journal of the American Chemical Society 118*, 1295-1301.

(25) Mohler, M. L., Cox, J. R., and Serpersu, E. H. (1998) Aminoglycoside phosphotransferase(3')-IIIa (APH(3')-IIIa)-bound conformation of the aminoglycoside lividomycin A characterized by NMR. *Carbohyd. Lett. 3*, 17-24.

PART II: THERMODYNAMICS OF AMINOGLYCOSIDE BINDING TO AMINOGLYCOSIDE-3′-PHOSPHOTRANSFERASE IIIA STUDIED BY ISOTHERMAL TITRATION CALORIMETRY

This section is a slightly revised version of a manuscript by Can Özen and Engin H. Serpersu published in *Biochemistry* in 2004:

Özen, C., and Serpersu, E. H. (2004) Thermodynamics of aminoglycoside binding to aminoglycoside-3′-phosphotransferase IIIa studied by isothermal titration calorimetry, *Biochemistry*. *43*, 14667–14675.

Abstract

The aminoglycoside-3′-phosphotransferase IIIa [APH(3′)-IIIa] phosphorylates aminoglycoside antibiotics and renders them ineffective against bacteria. APH(3′)-IIIa is the most promiscuous aminoglycoside phosphotransferase enzyme, and it modifies more than 10 different aminoglycoside antibiotics. A wealth of information exists about the enzyme; however, thermodynamic properties of enzyme–aminoglycoside complexes are still not known. This study describes the determination of the thermodynamic parameters of the binary enzyme–aminoglycoside and the ternary enzyme–metal-ATP–aminoglycoside complexes of structurally related aminoglycosides using isothermal titration calorimetry. Formation of the binary enzyme–aminoglycoside complexes is enthalpically driven and exhibits a strongly disfavored entropic contribution. Formation of the ternary enzyme–metal-ATP–aminoglycoside complexes yields much smaller negative ΔH values and more favorable entropic contributions. The presence of metal-ATP generally increases the affinity of aminoglycosides to the enzyme. This is consistent with the kinetic mechanism of the enzyme in which ordered binding of substrates occurs. However, the observed ΔH values correlate with neither kinetic parameters k_{cat}, K_m, and

k_{cat}/K_m nor with the molecular size of the substrates. Comparison of the thermodynamic properties of the complexes formed by structurally similar aminoglycosides indicated that the 2′- and the 6′-amino groups of the substrates are involved in binding to the enzyme. Thermodynamic properties of the complexes formed by aminoglycosides differing only at the 3′-hydroxyl group suggested that the absence of this group does not alter the thermodynamic parameters of the ternary APH(3′)-IIIa–metal-ATP–aminoglycoside complex. Our results also indicate that protonation of ligand and protein ionizable groups is coupled to the complex formation between aminoglycosides and APH(3′)-IIIa. Comparison of ΔH values for different aminoglycoside–enzyme complexes indicates that enzyme and substrates undergo significant conformational changes in complex formation.

Materials and Methods

Aminoglycoside antibiotics, adenosine 5′-triphosphate (ATP), and all other chemicals were of highest available purity and were obtained from Sigma (St. Louis, MO). The strong anion-exchange medium POROS 20HQ was purchased from Applied Biosystems (Foster City, CA).

Protein Purification. APH(3′)-IIIa was expressed in *Escherichia coli* BL21(DE3) carrying the overexpression plasmid pETPCR6, which was provided by Dr. Gerard D. Wright. APH(3′)-IIIa was purified using a modified version of the original procedure described by McKay et al. (*1*). Ten liters of Luria broth (LB) media in a New Brunswick (Edison, NJ) BioFlo 110 fermentor vessel was inoculated with a 100 mL overnight grown subculture. The cells were grown at 37 °C. The culture was induced at the mid log phase (OD_{600} = 0.6) with 1 mM final concentration of IPTG. After a 5 h induction period, the culture was divided into 1.5 L fractions, and then the cells were harvested by centrifugation. Each fraction was solubilized in 35 mL of lysis buffer (50 mM Tris, 5 mM EDTA, 200 mM NaCl, 1 mM PMSF, 0.2 mM DTT) and lysed by three to four passages through a French press at 16000 psi. Cell debris was removed by centrifugation, and the supernatant was diluted to 50 mL with buffer A (50 mM Tris, 1 mM EDTA, pH 8.0) before loading it onto a strong anion-exchange POROS 20HQ column (250 x 4.6 mm) attached to a BIOCAD 700E perfusion chromatography workstation from Applied Biosystems. After the cell hydrolysate was loaded, the column was washed with four column volumes of buffer A. A linear gradient of 0-20% buffer B in buffer A was applied through five column volumes to elute contaminant proteins. The pure APH(3′)-IIIa was then eluted with two column volumes of 20% buffer B in buffer A. Pooled fractions were

dialyzed against buffer A, freeze-dried, and stored at –80 °C. The purity of the enzyme was >98% as judged by SDS–PAGE. The activity of the enzyme was determined by using a coupled-enzyme assay as described previously (*1*).

ITC Experiments. Isothermal titration calorimetry experiments were performed at 37 °C using a VP-ITC microcalorimeter from Microcal, Inc. (Northampton, MA). Measurements were carried out in 50 mM Tris or Bicine buffers which also contained 100 mM KCl at pH values of 7.5 and 8.5. Enzyme preparations were dialyzed extensively against buffer, and ligand solutions were prepared in the final dialyzate. Both solutions were degassed under vacuum for 10 min. Titrations consisted of 29 injections programmed as 10 μL per injection and separated by 240 s. Cell stirring speed was 300 rpm.

Binary complex titrations were performed by titrating 0.75–3.0 mM aminoglycoside solution into a solution containing 50-100 μM APH(3′)-IIIa in the sample cell. To obtain reliable dissociation constants, the *c*-value, a parameter obtained by the multiplication of the association constant and the total concentration of ligand binding sites (*2*), was kept between 10 and 100 for all titrations. Due to tight binding of neomycin B and paromomycin I (*c*-values were ~600 at 80 μM enzyme concentration), the ternary titrations with these antibiotics were repeated at 10 μM enzyme concentration for more accurate determination of the dissociation constants. $CaCl_2$ (1.5 mM) and ATP (1.0 mM) were present in the syringe and sample cell during ternary complex titrations. Control runs were performed by titrating ligands to buffer, and the resulting reference signal was subtracted from corresponding experimental data. The enzymatic activity of APH(3′)-IIIa was tested before and after titrations, and no loss of activity was detected.

Thermodynamic parameters N (stoichiometry), K_A (association constant), and ΔH (enthalpy change) were obtained by nonlinear least-squares fitting of experimental data using a single-site binding model of the Origin software package (version 5.0) provided with the instrument. The free energy of binding (ΔG) and entropy change (ΔS) were obtained using the equations:

$$\Delta G = -RT \ln K_A \quad (1)$$

$$\Delta G = \Delta H - T\Delta S \quad (2)$$

The affinity of the aminoglycoside to the enzyme and enzyme–CaATP complex is given as the dissociation constant ($K_D = 1/K_A$). CaATP, a competitive inhibitor of the enzyme (*3*), was used instead of MgATP to prevent product formation in the ternary titrations.

Results and Discussion

ITC is a direct method for characterizing the stoichiometry, affinity, and enthalpy of binding reactions in solution (*4–6*) and has been employed in binding studies of saccharides with their partner lectins (*7–9*) or proteins (*10*), or aminoglycoside–RNA complexes (*11*), aminoglycoside–acetyltransferase interactions (*12*), and nucleotide binding to APH(3′)-IIIa (*13*). In this study, we used ITC to determine the thermodynamic parameters for aminoglycoside binding to APH(3′)-IIIa in the presence and absence of CaATP. Several aminoglycosides with 4,5- and 4,6-disubstituted 2-deoxystreptamine rings were used in binding studies (Part I Figure 1).

In general, the binding of aminoglycosides to APH(3′)-IIIa is an enthalpically driven process accompanied by an unfavorable entropic contribution. Negative ΔH values associated with the formation of binary APH(3′)-IIIa–aminoglycoside and ternary APH(3′)-IIIa–CaATP–aminoglycoside complexes suggest that favorable binding contacts such as polar, electrostatic, van der Waals, and hydrogen bonds exist between aminoglycosides and APH(3′)-IIIa. Exothermic heat and binding affinities were not, however, proportional with the size of aminoglycosides (i.e., larger aminoglycosides did not necessarily exhibit greater heats of association or tighter binding). Also, there was no correlation between the heat of binding and the kinetic parameters K_m, k_{cat}, or k_{cat}/K_m.

Binary Enzyme–Aminoglycoside Complexes. Calorimetric titration results show that formation of APH(3′)-IIIa–aminoglycoside complexes exhibits large, exothermic heats of association, and they are entropically disfavored (Table 1). This observation indicates that the sum of the total binding entropy due to solvation effects and to the rotational, translational, and configurational freedoms of aminoglycosides and

Table 1. Thermodynamic Parameters for Aminoglycoside Binding to APH(3′)-IIIa (Binary Complex) at pH 7.5[a]

	Buffer	K_D (μM)	ΔH_{obs} (kcal/mol)	ΔH_{int}[b] (kcal/mol)	$-T\Delta S$ (kcal/mol)	ΔG (kcal/mol)
Kanamycin A	TRIS	6.2	–33.0	–44.9	25.6	–7.4
	Bicine	4.6	–38.3		30.8	–7.5
Kanamycin B	TRIS	0.3	–22.4	–41.3	13.2	–9.2
	Bicine	0.5	–30.8		21.8	–9.0
Tobramycin	TRIS	0.8	–29.2	–47.0	20.5	–8.7
	Bicine	0.6	–37.1		28.3	–8.8
Amikacin	TRIS	92.6	–19.5	–17.9	13.8	–5.7
	Bicine	43.5	–18.8		12.6	–6.2
Ribostamycin	TRIS	1.7	–30.1	–25.6	22.0	–8.1
	Bicine	1.9	–28.1		20.0	–8.1
Neomycin B	TRIS	0.26	–33.4	–55.7	24.1	–9.3
	Bicine	0.30	–43.3		34.0	–9.3
Paromomycin I	TRIS	0.44	–30.4	–43.9	21.4	–9.0
	Bicine	0.30	–36.4		27.1	–9.3
Lividomycin A	TRIS	0.81	–33.6	–57.3	25.0	–8.6
	Bicine	0.57	–44.1		35.3	–8.8

[a] Determined at 310 K. K_D values were calculated from ITC-derived K_A. Fitting Errors: K_D, 2–12%; ΔH, 0.2–3%. The stoichiometry of complex formation was 1.0 ± 0.2 in all titrations. [b] Intrinsic enthalpy changes (ΔH_{int}) were calculated using eqs 3a and 3b.

APH(3′)- IIIa was greatly reduced as a result of complex formation. However, the large exothermic heats of association compensate for the entropic penalty to yield negative ΔG values in each case. In all cases, the best fits were obtained with a single-site model. Figure 1 shows the titration isotherms obtained for binary titrations of APH(3′)-IIIa with the tightest (neomycin B) and the weakest (amikacin) binding aminoglycosides. The differences between the heats of association and the binding affinities of the two aminoglycosides are clearly visible in this figure.

There were no clear trends with respect to dissociation constant (K_D) or other thermodynamic parameters to distinguish aminoglycosides with the 4,5- or 4,6-disubstituted 2-DOS rings from each other. While K_D values varied ~400-fold, ΔH_{obs} values were between –18.8 and –44.1 kcal/mol, and $T\Delta S$ values were between –12.6 and –35.3 kcal/mol. Overall, however, all binary enzyme–aminoglycoside complexes gave negative ΔG values. Also, with the exception of amikacin, all ΔG values were within 1.8 kcal/mol. The results observed with amikacin are somewhat expected since amikacin is one of the worst substrates of APH(3′)-IIIa (high K_m, low k_{cat}, and k_{cat}/K_m), with the lowest affinity and the smallest negative ΔG among the aminoglycosides tested. Amikacin has a bulky group attached to the N-1 of the 2-DOS ring (Part I Figure 1), which may interfere with the interaction of aminoglycoside with the enzyme. This may explain why amikacin is still a clinically useful antibiotic.

Observed ΔH values were different for the same complex when titrations were performed in buffers with different heats of ionization [Tris, 11.7 kcal/mol (*14*), vs Bicine, 6.5 kcal/mol (*15*)]. This observation indicates that the formation of enzyme–aminoglycoside complexes causes shifts in the pK_a values of ionizable groups and further

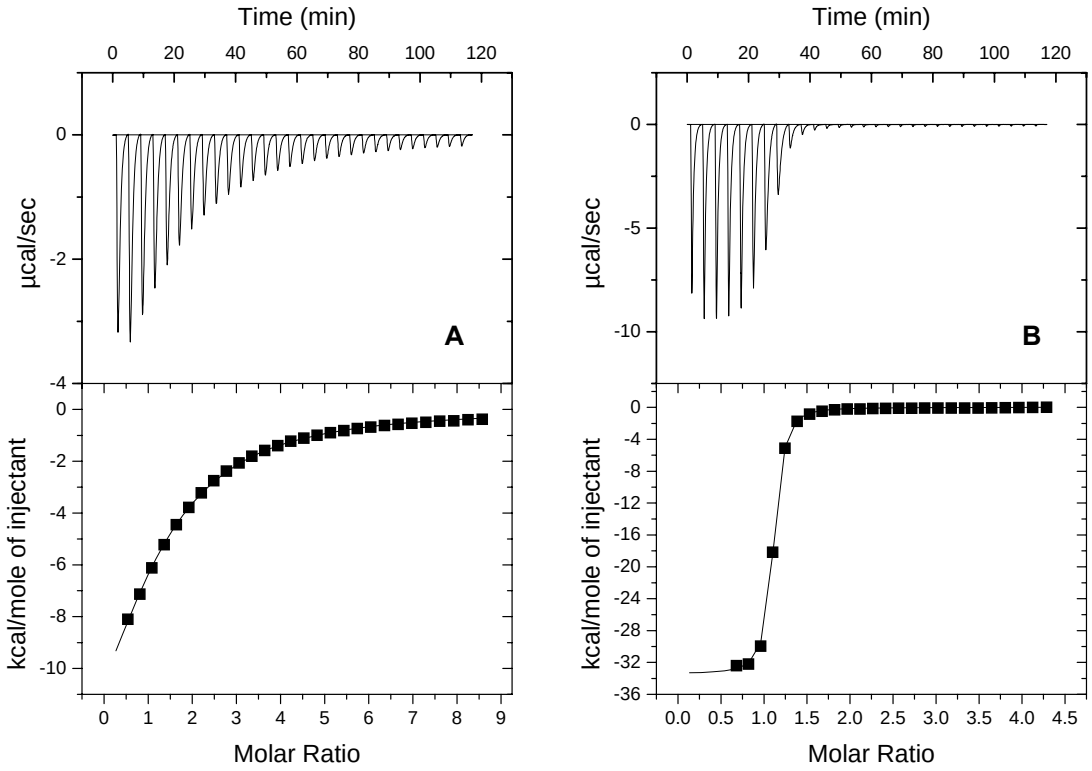

Figure 1. Isotherms of (A) 3.0 mM amikacin and (B) 1.5 mM neomycin B titration to 80 μM APH(3′)-IIIa. All solutions contained 50 mM Tris, pH 7.5, and 100 mM KCl, and titrations were performed at 310 K. The upper panel shows the raw data (thermal power). Time integration of the thermal power yields the heat of injection, which is plotted against the molar ratio of ligand to enzyme in the lower panel. The solid line in bottom panel represents the least-squares fitting of the data to a one-site binding model.

protonation/deprotonation occurs in the complex. The data obtained in two different buffers can then be used to determine the intrinsic enthalpy changes (ΔH_{int}) and net number of binding-coupled protons (Δn) for aminoglycoside–APH binary complex formation. These values were calculated by simultaneous solution of the equations (*16*):

$$\Delta H_{obs1} = \Delta H_{int} + \Delta H_{ion1}\Delta n \quad (3a)$$

$$\Delta H_{obs2} = \Delta H_{int} + \Delta H_{ion2}\Delta n \quad (3b)$$

where ΔH_{obs} is the observed enthalpy change, ΔH_{ion} is the ionization enthalpy change for the particular buffer used, and Δn is the net number of protons released or absorbed by the buffer upon complex formation. Positive values of the determined Δn for the formation of the binary enzyme–aminoglycoside complexes with kanamycin A, kanamycin B, tobramycin, neomycin B, paramomycin, and lividomycin A indicate binding-coupled protonation whereas negative values observed for ribostamycin and amikacin are due to the deprotonation of ligand and/or protein groups.

The data shown in Table 1 also indicates that ΔH_{int} values show a large variation for different aminoglycosides (more than ~3-fold). In addition, as shown in Table 2, the observed Δn values for the binary enzyme–aminoglycoside complexes with neomycin B and lividomycin A exceed the total fraction of $-NH_2$ groups on these ligands. Thus, additional protonation must occur in the enzyme side chains. Also, comparison of Δn values of kanamycin A and kanamycin B shows that the difference ($\Delta\Delta n$) is 0.6. The only difference between these two antibiotics is the presence of an amino (kanamycin B) vs hydroxyl (kanamycin A) at the 2′-position. However, the protonation of this group alone cannot be responsible for the observed Δn with kanamycin B, because it is already 92% protonated at pH 7.5. Similarly, the comparison of the complexes of neomycin B and

ribostamycin shows a $\Delta\Delta n$ value of 2.28, which exceeds the differences in the fraction of $-NH_2$ groups of the two antibiotics. These observations suggest that not only does the ionization of enzyme side chains contribute to the observed heat of the complex formation, but the contribution is different for each aminoglycoside. These are in excellent agreement with the results obtained by NMR studies. Heteronuclear $^{1}H-^{15}N$ HSQC spectra acquired with enzyme–aminoglycoside complexes using ^{15}N-enriched enzyme showed that different sets of backbone amide resonances were shifted with each aminoglycoside, suggesting that the conformation of the active site is altered to accommodate each aminoglycoside (Whittemore and Serpersu, unpublished data). Thus, the contribution of the enzyme to the determined ΔH_{int} may be different for each aminoglycoside.

Ternary Enzyme–CaATP–Aminoglycoside Complexes. An exothermic heat also accompanied titration of aminoglycosides into the enzyme–CaATP complex. However, the observed heat was significantly lower than the ΔH values observed in the binary titrations. As shown in Figure 2, the titration of ribostamycin into the solutions containing enzyme alone or the enzyme–CaATP complex exhibits different patterns. Comparison of aminoglycoside binding to APH(3′)-IIIa shows that binding is generally tighter or unchanged in the presence of CaATP (Tables 1 and 3).These results are in agreement with previous steady-state kinetics, viscosity, thio, and solvent isotope effect studies (*19*, *20*) suggesting a special case of ordered Bi-Bi kinetic model for APH(3′)-IIIa called Theorell–Chance mechanism in which ATP binds first with rapid equilibrium followed by aminoglycoside binding, release of phosphorylated aminoglycoside and lastly release of ADP (rate limiting step). It can also be suggested that the large exothermic heats

Table 2. Protonation Coupled to Aminoglycoside Binding to APH(3′)-IIIa (Binary Complex) at pH 7.5

	Total Fraction of NH_2[a]	Δn[b]
Kanamycin A	2.51	1.02
Kanamycin B	2.59	1.62
Tobramycin	2.59	1.52
Amikacin	1.25	–0.13
Ribostamycin	1.71	–0.38
Neomycin B	1.15	1.90
Paromomycin I	1.18	1.15
Lividomycin A	1.14	2.03

[a] The total fraction of deprotonated amino groups was calculated on the basis of the determined pK_a values of aminoglycosides (*11, 17, 18*). [b] The net number of binding-coupled protons was calculated using eqs 3a and 3b.

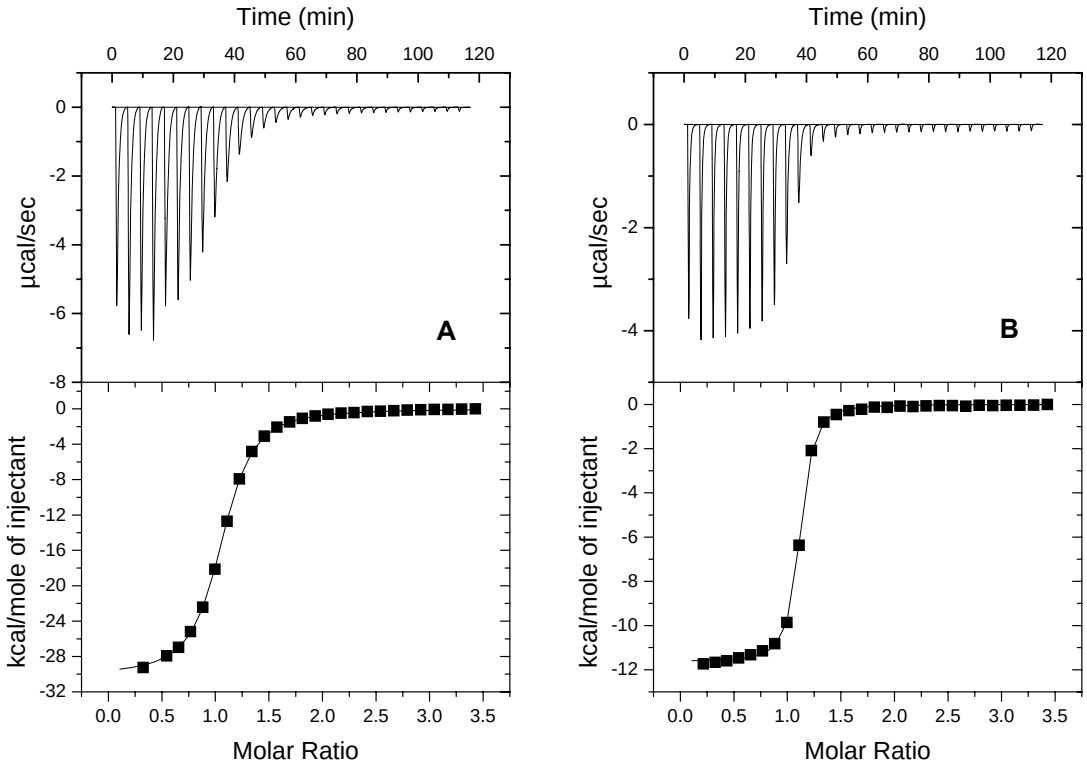

Figure 2. ITC profiles of 1.2 mM ribostamycin titration to 80 μM APH(3′)-IIIa in the absence (A) and presence (B) of CaATP. Other experimental conditions were as described in Figure 1. The raw data are shown in the upper panels, and plots of the heat of injection against the molar ratio of ligand to enzyme are shown in the lower panels with the best-fit lines to a one-site model. The steeper saturation curve in (B) yields more than a 6-fold higher association constant for the complex formation.

Table 3. Thermodynamic Parameters for Aminoglycoside Binding to APH(3′)-IIIa–CaATP (Ternary Complex) at pH 7.5[a]

	Buffer	K_D (μM)	ΔH_{obs} (kcal/mol)	ΔH_{int}[b] (kcal/mol)	$-T\Delta S$ (kcal/mol)	ΔG (kcal/mol)	Δn[b]
Kanamycin A	TRIS	0.99	–9.4	–31.0	0.9	–8.5	1.85
	Bicine	1.3	–19.0		10.7	–8.3	
Kanamycin B	TRIS	0.22	–8.2	–29.1	–1.2	–9.4	1.79
	Bicine	0.39	–17.5		8.4	–9.1	
Tobramycin	TRIS	0.22	–9.1	–30.7	–0.3	–9.4	1.85
	Bicine	0.55	–18.7		9.8	–8.9	
Amikacin	TRIS	33.3	–4.8	–28.0	–1.5	–6.3	1.98
	Bicine	25.7	–15.1		8.6	–6.5	
Ribostamycin	TRIS	0.27	–11.6	–14.5	2.3	–9.3	0.25
	Bicine	0.53	–12.9		4.0	–8.9	
Neomycin B	TRIS	0.13	–12.2	–36.3	2.4	–9.8	2.06
	Bicine	0.30	–22.9		13.6	–9.3	
Paromomycin I	TRIS	0.16	–11.5	–27.9	1.8	–9.7	1.40
	Bicine	0.12	–18.8		9.0	–9.8	
Lividomycin A	TRIS	0.78	–10.5	–36.6	1.8	–8.7	2.23
	Bicine	0.55	–22.1		13.2	–8.9	

[a] Determined at 310 K. K_D values were calculated from ITC-derived K_A. Fitting Errors: K_D, 2–12%; ΔH, 0.2–3%. The stoichiometry of complex formation was 1.0 ± 0.2 in all titrations. [b] Intrinsic enthalpy changes (ΔH_{int}) and net number of binding-coupled protons (Δn) were calculated using eqs 3a and 3b.

observed in the formation of the binary enzyme–aminoglycoside complexes were mostly due to conformational changes in enzyme or ligand or both. Our earlier work showed that the enzyme-bound aminoglycosides, unlike their unbound forms, do not necessarily adopt the lowest energy conformation (*21*, *22*).Thus, enzyme binding causes conformational changes in aminoglycosides. In addition, NMR spectra acquired with enzyme, enzyme–CaATP,enzyme–aminoglycoside, and enzyme–CaATP–aminoglycoside complexes,using uniformly ^{15}N-enriched APH(3′)-IIIa, showed that the binding of aminoglycosides to the APH(3′)-IIIa or APH(3′)-IIIa–CaATP caused a larger number of backbone resonances to shift when compared to the addition of CaATP to the enzyme or enzyme–aminoglycoside complex, suggesting that the binding of aminoglycoside causes significant conformational changes in the enzyme (Whittemore and Serpersu, unpublished data).

In the ternary complex formation, as was the case with the binary complexes, there were no trends separating the aminoglycosides with 4,5-disubstituted 2-DOS from those with 4,6-disubstituted 2-DOS with respect to the thermodynamic parameters. Overall, the entropic contribution was more favorable in the ternary complexes with all aminoglycosides when compared to the respective binary complexes. An explanation for this observation can be that the binding in the ternary complex is accompanied by expulsion of more water molecules from the binding interface when compared to the binary aminoglycoside–enzyme interaction. Thus, gain in entropy of the freed water molecules would provide a more favorable driving force for the formation of the ternary complex. Alternatively, the more favorable entropic contribution may come from the increased hydrophobic interactions between the enzyme and the ligands. It is already shown in the crystal structure of the enzyme with substrates (*23*) that the adenine moiety

of MgADP is involved in a stacking interaction with the aromatic ring of the Tyr 42. This interaction is absent in the binary enzyme–aminoglycoside complex.

The spread between the lowest and highest affinity toward the enzyme was somewhat narrower in ternary complexes. Overall, ΔG values for each antibiotic were only slightly more negative in the ternary complexes when compared to the respective binary complexes. In the ternary complexes, more uniform Δn values were obtained, and the values of ΔH_{int} varied between –14.5 and –36.6 kcal/mol. The analysis of these values, however, is even more complicated than those of the binary complexes due to contributions that may result from the interactions of ATP with protein and ligand coordination to the metal ion. On the other hand, comparison of the dissociation constants of various enzyme–aminoglycoside complexes (a thermodynamic property which is not directly correlated to the heat of reaction) with several aminoglycosides that have a structural difference of either a single functional group or a complete sugar ring between two aminoglycosides afforded some clues about the roles of these groups in enzyme–aminoglycoside interactions. Several specific comparisons are presented in the following paragraphs.

2′-Amino vs Hydroxyl. Kanamycin A and kanamycin B differ only by the presence of an amino group at the 2′-position of kanamycin B instead of the hydroxyl in kanamycin A (Part I Figure 1). ΔH_{int} is 3.6 kcal/mol less negative with kanamycin B when compared to kanamycin A in the binary enzyme–aminoglycoside complex (Table 1), while the affinity of kanamycin B to the enzyme is ~15-fold higher than that of kanamycin A. These differences between the kanamycins are significantly reduced in the ternary complexes (Table 3). If one assumes the ability of the protonated (or

unprotonated) amino group to form stronger hydrogen bonds than the hydroxyl group, then the expected ΔH should have been more negative with kanamycin B. On the other hand, increased strength of additional hydrogen bonds mediated by the 2′-amino group may weaken other favorable interactions, i.e., altered cooperativity among hydrogen bonds, causing a less enthalphically driven complex formation for kanamycin B. Alternatively, the more negative ΔH with kanamycin A may be the result of larger conformational changes in enzyme or antibiotic or both. If the protonated amino group is involved in ionic interactions with the protein side chains, then this would provide more positive entropic contribution to the binding through desolvation. The second alternative appears to account for the relatively more favorable entropic terms in the binary and ternary complexes of kanamycin B with respect to kanamycin A.

A crystal structure for the binary kanamycin–APH(3′)-IIIa complex is not available; however, the crystal structure of the ternary APH(3′)-IIIa–MgADP–kanamycin A complex is available (*23*). Examination of the crystal structure reveals that the closest enzyme atom to the 2′-hydroxyl oxygen is the side chain carboxyl oxygen of Asp 190 at a distance of 4.2 Å in the ternary complex (Figure 3), and therefore the 2′-position was not considered among the enzyme contacts in previous structural analyses (*23*). The pK_a of the 2′-amino group is ~8.6 (*18*), which is the highest of all amine groups on kanamycin B. At pH 7.5 only the 2′-amino group would be ~90% protonated while all others would be ~50% or less protonated. Experiments performed with the ternary complexes at pH 8.5 (Figure 4) showed that ΔH_{int} for kanamycin A was only slighty changed, while it became significantly more negative for kanamycin B. The entropic contributions were reversed in both cases and became more disfavored with kanamycin B (Table 4). At this pH only the

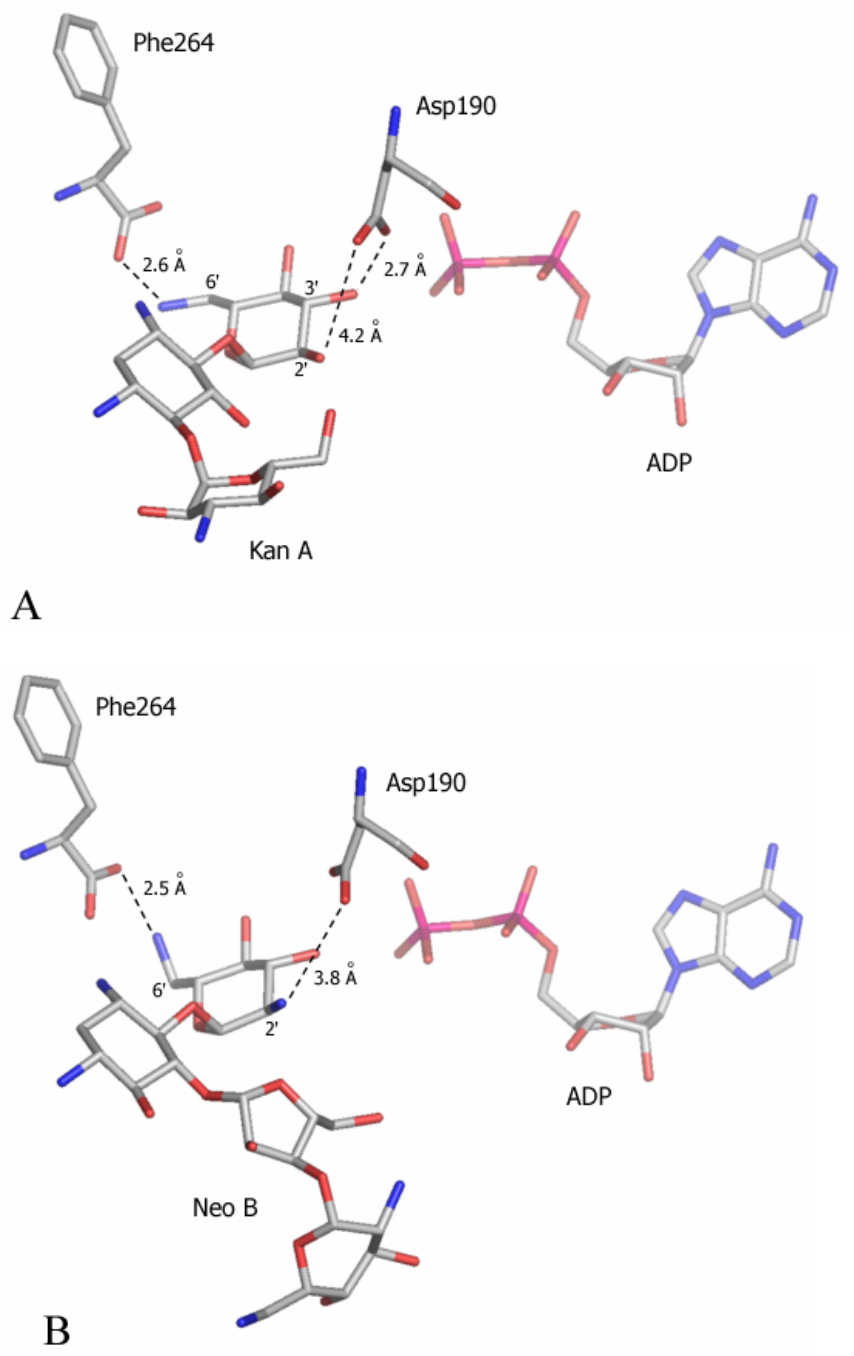

Figure 3. Crystal structures of (A) kanamycin A and (B) neomycin B complexed with ADP and APH(3′)-IIIa (*23*). Images were produced by Deep View (*24*) and Pymol (*25*). The relevant distances between ligand functional groups and enzyme residues are indicated with dotted lines.

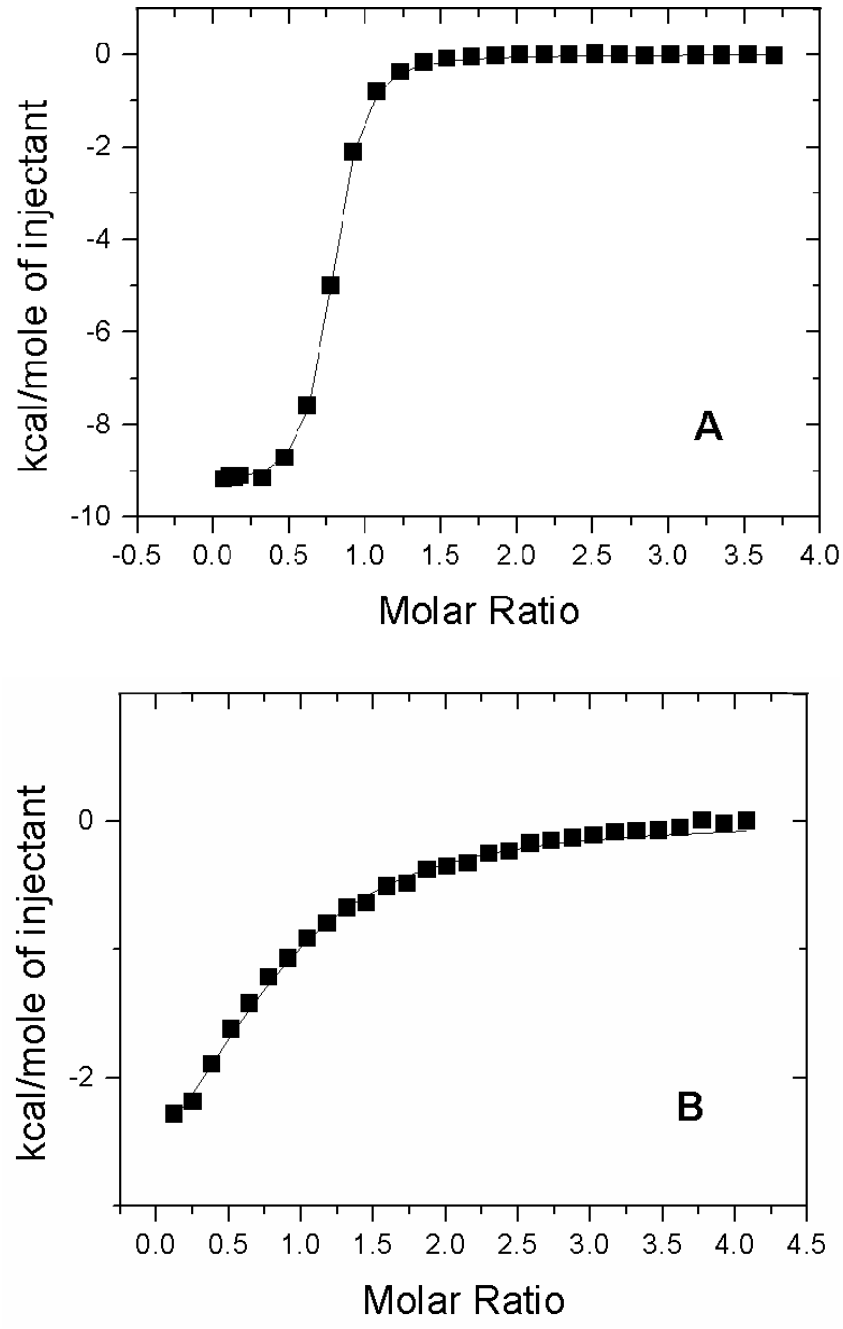

Figure 4. Heat of injection observed in the titration of kanamycin A to 80 μM APH(3′)-IIIa in the presence of CaATP at pH 7.5 (A) and 8.5 (B). Other experimental conditions were as described in Figure 1. The solid line represents the best fit to the data using a one-site binding model.

Table 4. Thermodynamic Parameters for Aminoglycoside Binding to APH(3′)-IIIa–CaATP (Ternary Complex) at pH 8.5[a]

	Buffer	K_D (μM)	ΔH_{obs} (kcal/mol)	ΔH_{int}[b] (kcal/mol)	$-T\Delta S$ (kcal/mol)	ΔG (kcal/mol)	Δn[b]
Kanamycin A	TRIS	28.3	–3.7	–34.1	–2.8	–6.5	2.60
	Bicine	24.2	–17.2		10.7	–6.5	
Kanamycin B	TRIS	9.4	–8.5	–48.3	1.3	–7.1	3.40
	Bicine	4.4	–26.2		18.6	–7.6	
Tobramycin	TRIS	12.6	–7.0	–48.4	0.09	–7.0	3.54
	Bicine	5.6	–25.4		18.0	–7.4	
Neomycin B	TRIS	0.40	–11.1	–55.7	2.2	–8.9	3.81
	Bicine	0.17	–30.9		21.3	–9.6	
Paromomycin I	TRIS	3.7	–10.9	–48.9	3.1	–7.8	3.25
	Bicine	1.88	–27.8		19.7	–8.1	

[a] Determined at 310 K. K_D values were calculated from ITC-derived K_A. Fitting Errors: K_D, 2–10%; ΔH, 0.5–6%. The stoichiometry of complex formation was 1.0 ± 0.2 in all titrations. [b] Intrinsic enthalpy changes (ΔH_{int}) and net number of binding-coupled protons (Δn) were calculated using eqs 3a and 3b.

2′-amino group of unbound kanamycin B would be ~50% protonated while the others are only ~10% protonated. Since kanamycin A lacks the 2′-amino group, at pH 8.5, all of its amino groups would be only about 10% protonated. This suggests that charged amino groups of aminoglycosides provide favorable binding interactions in enzyme–aminoglycoside complexes.

These observations are also consistent with the involvement of the charged 2′-amino group in enzyme–kanamycin B interactions. The determined $\Delta\Delta n$ value between the kanamycins is 0.8 at pH 8.5. This value, again, exceeds the total protonation capacity of the 2′-amino group and suggests that other groups must be involved. These results also suggest that even very small structural differences between ligands may alter other enzyme–ligand interactions involving the similar structural parts of ligands (i.e., increased or decreased cooperativity among the hydrogen bonds). Thus observed changes in the thermodynamic parameters may not easily be reconciled in a quantitative manner.

6′-Amino vs Hydroxyl. The presence of an amino or hydroxyl group at the 6′-position is the only difference between neomycin B (amine) and paromomycin I (hydroxyl) (Part I Figure 1). Binary complexes of both aminoglycosides with the enzyme exhibit similar K_D values, but their intrinsic binding enthalpies differ by 13.4 kcal/mol (Table 1). However, when the ternary titrations were performed at pH 8.5, at which only the 6′-amino group would be ~50% protonated while the others are in a ~10% protonated state, significant differences were observed between the binding pattern of the two antibiotics. The dissociation constant of paromomycin I from the ternary APH(3′)-IIIa–CaATP–paromomycin I complex was increased by ~20-fold, while the same effect was only 1.3-fold for neomycin B. This observation suggests that the remaining charge on the

6′-amino group of neomycin B is responsible for the ~10-fold tighter binding of this antibiotic to the enzyme when compared to paromomycin I at pH 8.5. Thus, the 6′-amino group must be involved in enzyme–aminoglycoside interactions, and it contributes 1.3 kcal/mol favorably to ΔG when it is in the ~50% protonated state. Although the determined $\Delta\Delta n$ value of 0.56 can be attributed to the protonation of the 6′-amino group alone, as indicated above, this may be coincidental, and contributions due to protonation/deprotonation of other groups cannot be ruled out.

The crystal structure of the ternary APH(3′)-IIIa–MgADP–neomycin B complex shows that the 6′-amino group is 2.6 Å away from one of the carboxyl oxygens of the C-terminal residue Phe 264 (Figure 3). Entropic contributions are similar in the ternary complexes of neomycin B and paramomycin I at pH 8.5. Thus, the observed difference in ΔG is solely due to the difference in ΔH, and it may reflect the ability of the amino group to form stronger hydrogen bonds than the hydroxyl group with Phe 264.

The importance of the 2′- and the 6′-amino groups is also supported by the chemical modification studies in which particular amino groups were one-by-one deaminated to study their role in enzyme catalysis (*26*). Elimination of the 2′-and the 6′-amino groups was shown to increase K_m and bring about 10- and 30-fold losses of catalytic efficiency of APH(3′)-IIIa, respectively. In this work, we showed that even replacement of these amino groups by hydroxyl groups still shows significant effects on the thermodynamic properties of the binary and ternary enzyme–aminoglycoside complexes.

3′-Deoxy vs *Hydroxyl.* Tobramycin, a competitive inhibitor of APH(3′)-IIIa, lacks the 3′-hydroxyl group of kanamycin B and therefore cannot be modified by the enzyme.

Comparison of K_D for tobramycin and kanamycin B shows that the presence or absence of a hydroxyl group at the 3′-position does not have an effect on the affinity of aminoglycoside to the enzyme–metal-ATP complex. As was the case with kanamycin A vs kanamycin B, there were differences between the thermodynamic parameters of the binary complexes of kanamycin B and tobramycin with APH(3′)-IIIa (Table 1). Kanamycin B exhibited lower ΔH and $T\Delta S$ values in the binary complex. These differences disappeared almost completely in the ternary complexes, yielding not only identical ΔG and K_D values but also similar ΔH and $T\Delta S$ values (Table 3). These observations suggest that once the nucleotide-binding site is occupied, the 3′-hydroxyl group has no significant contribution to the thermodynamic parameters. This is somewhat surprising since the 3′-OH is the point of modification by APH(3′)-IIIa, and it is located near the catalytically required residue Asp 190 (Figure 3). Thus, one would expect this group to be positioned precisely for a nucleophilic attack on the γ-phosphoryl group of ATP via interaction(s) with Asp 190. A plausible explanation may be that the removal of the hydroxyl group leads to stronger interactions via other existing hydrogen bonds between the aminoglycoside and the enzyme and/or alters the organization of water in the active site, which compensates for the loss of a hydrogen bond through the 3′-hydroxyl. These results, again, clearly suggest that interpretation of thermodynamic data, even for very similar compounds, may not be straightforward, and detailed structural information on the complexes of each compound is necessary for a more quantitative interpretation.

Size of Substrates. Comparison of thermodynamic parameters of the binary and ternary complexes of ribostamycin (three rings), neomycinB/paramomycin I (four rings), and lividomycin A (five rings) shows that the determined ΔH_{int} is significantly different

for ribostamycin. Since ribostamycin is the smallest of them, these observations suggest that the fourth rings of the longer aminoglycosides contribute to binding. Examination of the data also yields that the fifth ring of lividomycin A does not contribute to binding. The crystal structure of the APH(3′)-IIIa–MgADP–neomycin B complex (*23*) shows that the side chain nitrogens and oxygens of Asn 134, Asp 193, Ser 194, and Glu 230 are within 4 Å distance of the fourth ring of neomycin B. Thus one or more of these side chains may interact with this ring.

Enthalpy–Entropy Compensation. The determined ΔH_{obs} and $T\Delta S$ values were plotted for the binary and the ternary complexes to investigate the enthalpy–entropy compensation of the aminoglycoside binding to APH(3′)-IIIa. Enthalpy–entropy compensation for the formation of the binary and ternary complexes of each aminoglycoside are shown in Figures 5 and 6. Plots of enthalpy–entropy compensation with a slope of unity indicate that changes in binding enthalpies ($\Delta\Delta H$) are equally compensated by changes in binding entropies ($\Delta\Delta S$) between the different ligands of an enzyme. If $\Delta\Delta H$ is greater than $\Delta\Delta S$, a slope greater than unity is obtained. In the case where $\Delta\Delta H$ is smaller than the $\Delta\Delta S$, the slope is smaller than unity. Such plots for binary and ternary complexes of APH(3′)-IIIa with substrates yielded slopes of 1.09 and 1.04, respectively (Figure 6), indicating that, in both cases, changes in binding enthalpies of different aminoglycosides are equally compensated by the changes in their entropic terms.

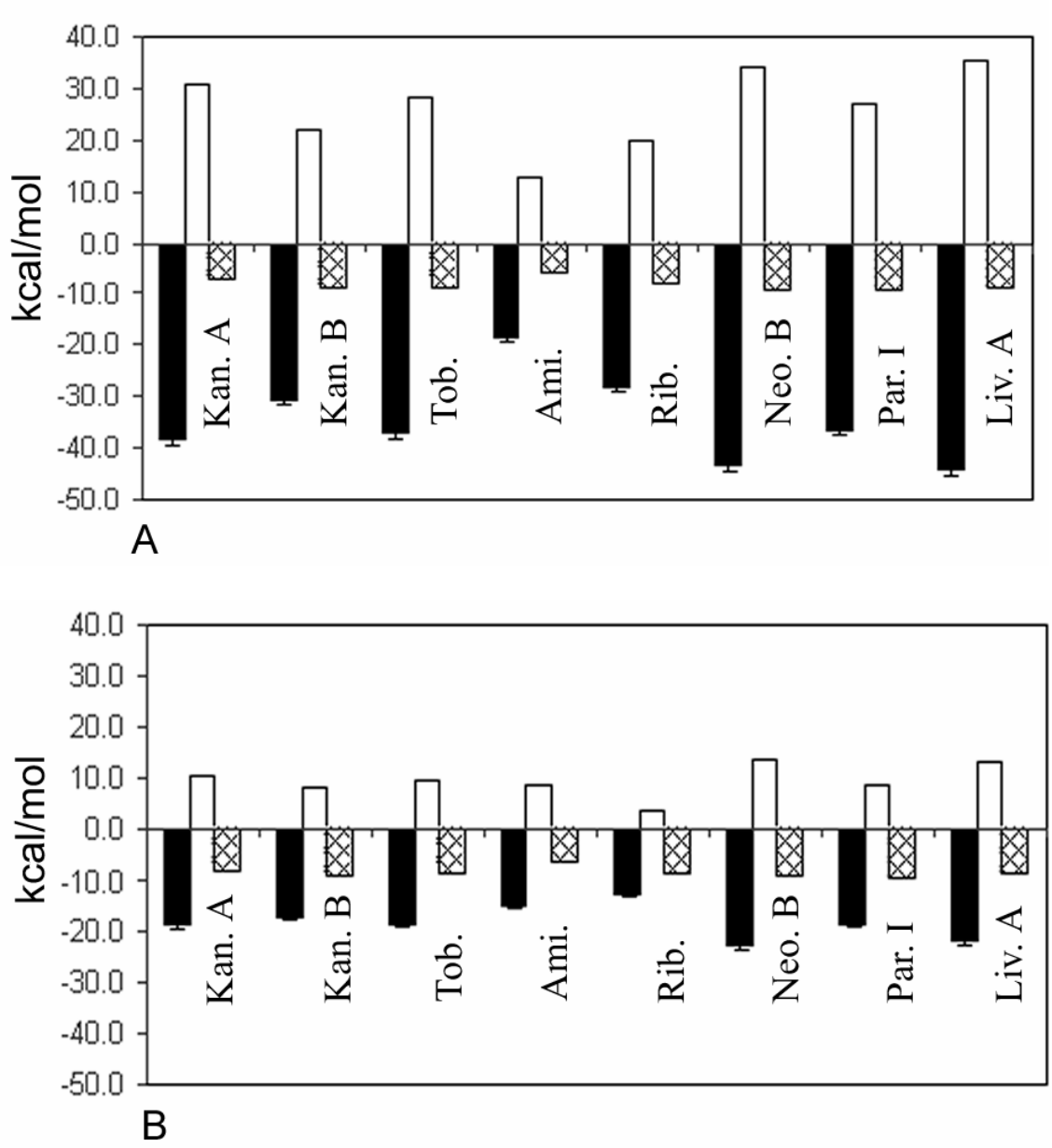

Figure 5. Thermodynamic parameters of aminoglycoside binding to (A) APH(3′)-IIIa and (B) the APH(3′)-IIIa–CaATP complex at 310 K in Bicine buffer. Bars represent Δ*H* (black*)*, –*T*Δ*S* (white), and Δ*G* (crossed). Abbreviations: Kan. A, kanamycin A; Kan. B, kanamycin B; Tob., tobramycin; Ami., amikacin; Rib., ribostamycin; Neo. B, neomycin B; Par. I, paromomycin I; Liv. A, lividomycin A.

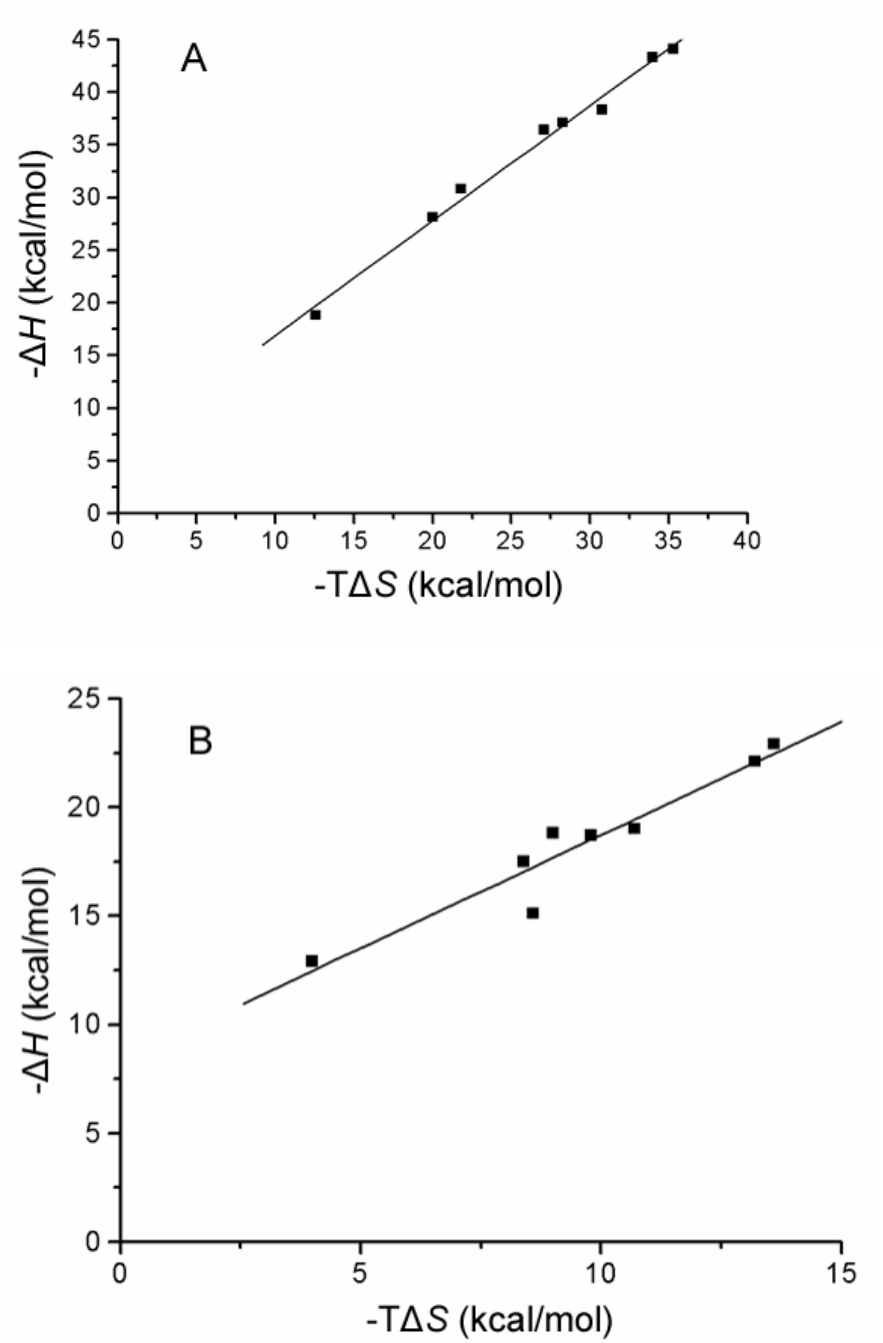

Figure 6. Enthalpy–entropy compensation plots constructed by linear regression analysis of binding data from Tables 1 and 3. (A) Binary enzyme–aminoglycoside complexes (slope = 1.09, R = 0.99) and (B) ternary enzyme–CaATP–aminoglycoside complexes (slope = 1.04, R = 0.96).

Conclusions

With the exception of amikacin, the free energies of formation for the binary enzyme–aminoglycoside and the ternary enzyme–CaATP–aminoglycoside complexes were similar to each other regardless of the structure of the aminoglycosides involved. The heat of formation and the entropic contribution to complex formation, however, showed significant variation among the aminoglycosides. The formation of all binary complexes exhibits large negative ΔH values with strongly disfavored entropic contribution. This is significantly different from the aminoglycoside–RNA interactions that show favorable entropic contribution to the complex formation (*11*). The formation of ternary complexes, on the other hand, was entropically more favored when compared to the binary complexes. Overall, there were no strong correlations between the thermodynamic parameters and the size of the aminoglycosides, or the kinetic parameters, or the substitution pattern of the 2-DOS ring (4,5 vs 4,6). Also, comparisons between structurally very similar aminoglycosides showed that the presence of an amino or hydroxyl group at the 2′- and the 6′-positions affected the thermodynamic properties of various enzyme–aminoglycoside complexes significantly, while the lack of a hydroxyl group at the 3′-position had no detectable effect. Similarly, additional sugar rings of larger aminoglycosides beyond the fourth ring appear to have no significant effect on the thermodynamic properties of enzyme–aminoglycoside complexes.

Acknowledgements

This research was supported by a grant from the National Science Foundation (MCB 01110741 to E.H.S.).

List of References

References

1. McKay, G. A., Thompson, P. R., and Wright, G. D. (1994) Broad spectrum aminoglycoside phosphotransferase type III from Enterococcus: overexpression, purification, and substrate specificity, *Biochemistry 33*, 6936-44.
2. Wiseman, T., Williston, S., Brandts, J. F., and Lin, L. N. (1989) Rapid measurement of binding constants and heats of binding using a new titration calorimeter, *Anal. Biochem. 179*, 131-7.
3. Cox, J. R., McKay, G. A., Wright, G. D., and Serpersu, E. H. (1996) Arrangement of substrates at the active site of an aminoglycoside antibiotic 3'-phosphotransferase as determined by NMR, *Journal of the American Chemical Society 118*, 1295-1301.
4. Ladbury, J. E., and Chowdhry, B. Z. (1996) Sensing the heat: the application of isothermal titration calorimetry to thermodynamic studies of biomolecular interactions, *Chem. Biol. 3*, 791-801.
5. Jelesarov, I., and Bosshard, H. R. (1999) Isothermal titration calorimetry and differential scanning calorimetry as complementary tools to investigate the energetics of biomolecular recognition, *J. Mol. Recognit. 12*, 3-18.
6. Leavitt, S., and Freire, E. (2001) Direct measurement of protein binding energetics by isothermal titration calorimetry, *Curr. Opin. Struct. Biol. 11*, 560-6.
7. Surolia, A., Sharon, N., and Schwarz, F. P. (1996) Thermodynamics of monosaccharide and disaccharide binding to Erythrina corallodendron lectin, *J. Biol. Chem. 271*, 17697-703.
8. Dam, T. K., and Brewer, C. F. (2002) Thermodynamic studies of lectin-carbohydrate interactions by isothermal titration calorimetry, *Chem. Rev. 102*, 387-429.
9. Chervenak, M. C., and Toone, E. J. (1995) Calorimetric analysis of the binding of lectins with overlapping carbohydrate-binding ligand specificities, *Biochemistry 34*, 5685-95.
10. Xie, H., Bolam, D. N., Nagy, T., Szabo, L., Cooper, A., Simpson, P. J., Lakey, J. H., Williamson, M. P., and Gilbert, H. J. (2001) Role of hydrogen bonding in the interaction between a xylan binding module and xylan, *Biochemistry 40*, 5700-7.
11. Kaul, M., Barbieri, C. M., Kerrigan, J. E., and Pilch, D. S. (2003) Coupling of drug protonation to the specific binding of aminoglycosides to the A site of 16 S rRNA: elucidation of the number of drug amino groups involved and their identities, *J. Mol. Biol. 326*, 1373-87.
12. Hegde, S. S., Dam, T. K., Brewer, C. F., and Blanchard, J. S. (2002) Thermodynamics of aminoglycoside and acyl-coenzyme A binding to the Salmonella enterica AAC(6')-Iy aminoglycoside N-acetyltransferase, *Biochemistry 41*, 7519-27.
13. Boehr, D. D., Farley, A. R., Wright, G. D., and Cox, J. R. (2002) Analysis of the pi-pi Stacking Interactions between the Aminoglycoside Antibiotic Kinase APH(3')-IIIa and Its Nucleotide Ligands, *Chem. Biol. 9*, 1209-17.
14. Bernhard, S. A. (1956) Ionization constants and heats of tris(hydroxymethyl)aminomethane and phosphate buffers, *J. Biol. Chem. 218*,

961-9.
15. Fukada, H., and Takahashi, K. (1998) Enthalpy and heat capacity changes for the proton dissociation of various buffer components in 0.1 M potassium chloride, *Proteins 33*, 159-66.
16. Doyle, M. L., Louie, G., Dal Monte, P. R., and Sokoloski, T. D. (1995) Tight binding affinities determined from thermodynamic linkage to protons by titration calorimetry, *Methods Enzymol. 259*, 183-94.
17. Cox, J. R., and Serpersu, E. H. (1997) Biologically important conformations of aminoglycoside antibiotics bound to an aminoglycoside 3'-phosphotransferase as determined by transferred nuclear Overhauser effect spectroscopy, *Biochemistry 36*, 2353-9.
18. Walter, F., Vicens, Q., and Westhof, E. (1999) Aminoglycoside-RNA interactions, *Curr. Opin. Chem. Biol. 3*, 694-704.
19. McKay, G. A., and Wright, G. D. (1995) Kinetic mechanism of aminoglycoside phosphotransferase type IIIa. Evidence for a Theorell-Chance mechanism, *J. Biol. Chem. 270*, 24686-92.
20. McKay, G. A., and Wright, G. D. (1996) Catalytic mechanism of enterococcal kanamycin kinase (APH(3')-IIIa): viscosity, thio, and solvent isotope effects support a Theorell-Chance mechanism, *Biochemistry 35*, 8680-5.
21. DiGiammarino, E. L., Draker, K. A., Wright, G. D., and Serpersu, E. H. (1998) Solution studies of isepamicin and conformational comparisons between isepamicin and butirosin A when bound to an aminoglycoside 6'-N-acetyltransferase determined by NMR spectroscopy, *Biochemistry 37*, 3638-44.
22. Mohler, M. L., Cox, J. R., and Serpersu, E. H. (1998) Aminoglycoside phosphotransferase(3')-IIIa (APH(3')-IIIa)-bound conformation of the aminoglycoside lividomycin A characterized by NMR, *Carbohyd. Lett. 3*, 17-24.
23. Fong, D. H., and Berghuis, A. M. (2002) Substrate promiscuity of an aminoglycoside antibiotic resistance enzyme via target mimicry, *Embo. J. 21*, 2323-31.
24. Guex, N., and Peitsch, M. C. (1997) SWISS-MODEL and the Swiss-PdbViewer: an environment for comparative protein modeling, *Electrophoresis 18*, 2714-23.
25. Delano, W. L. *The PyMol Molecular Graphics System;* DeLano Scientific: San Carlos, CA., 2002.
26. McKay, G. A., Roestamadji, J., Mobashery, S., and Wright, G. D. (1996) Recognition of aminoglycoside antibiotics by enterococcal-staphylococcal aminoglycoside 3'-phosphotransferase type IIIa: role of substrate amino groups, *Antimicrob. Agents Chemother. 40*, 2648-50.

PART III: DISSECTION OF AMINOGLYCOSIDE–ENZYME INTERACTIONS: A CALORIMETRIC AND NMR STUDY OF NEOMYCIN B BINDING TO THE AMINOGLYCOSIDE PHOSPHOTRANSFERASE(3′)-IIIA

This section is a slightly revised version of a manuscript by Can Özen, Joseph M. Malek, and Engin H. Serpersu published in *JACS* in 2006:

Özen, C., Malek, J. M., and Serpersu, E. H. (2006) Dissection of Aminoglycoside–Enzyme Interactions: A Calorimetric and NMR Study of Neomycin B Binding to the Aminoglycoside Phosphotransferase(3′)-IIIa, *JACS. 128*, 15248–15254.

Abstract

In this work, for the first time, we report pK_a values of the amino functions in a target-bound aminoglycoside antibiotic, which permitted dissection of the thermodynamic properties of an enzyme–aminoglycoside complex. Uniformly enriched ^{15}N-neomycin was isolated from cultures of *Streptomyces fradiae* and used to study its binding to the aminoglycoside phosphotransferase(3′)-IIIa (APH) by ^{15}N NMR spectroscopy. ^{15}N NMR studies showed that binding of neomycin to APH causes upshifts of ~1 pK_a unit for the amines N2′ and N2‴ while N6′ experienced a 0.3 pK_a unit shift. The pK_a of N6‴ remained unaltered, and resonances of N1 and N3 showed significant broadening upon binding to the enzyme. The binding-linked protonation and pH dependence of the association constant (K_b) for the enzyme–aminoglycoside complex was determined by isothermal titration calorimetry. The enthalpy of binding became more favorable (negative) with increasing pH. At high pH, binding-linked protonation was attributable mostly to the amino functions of neomycin; however, at neutral pH, functional groups of the enzyme, possibly remote from the active site, also underwent protonation/deprotonation upon formation of the binary enzyme–neomycin complex. The

K_b for the enzyme–neomycin complex showed a complicated dependence on pH, indicating that multiple interactions may affect the affinity of the ligand to the enzyme and altered conditions, such as pH, may favor one or another. This work highlights the importance of determining thermodynamic parameters of aminoglycoside–target interactions under different conditions before making attributions to specific sites and their effects on these global parameters.

Introduction

In this part, we present data obtained by direct measurement of the pK_a values of the amino groups of an aminoglycoside, neomycin, in an aminoglycoside–target complex. This data was used to dissect neomycin–enzyme interactions and determine contributions of individual amino groups of the ligand to the global thermodynamic properties of the enzyme–aminoglycoside complex. Our results show that binding of aminoglycosides to the enzyme causes upshifts in the pK_a values of amino groups on the ligand. However, the binding affinity of aminoglycosides to APH shows a complex dependence on pH, and increased positive charge on the aminoglycoside does not always increase the affinity.

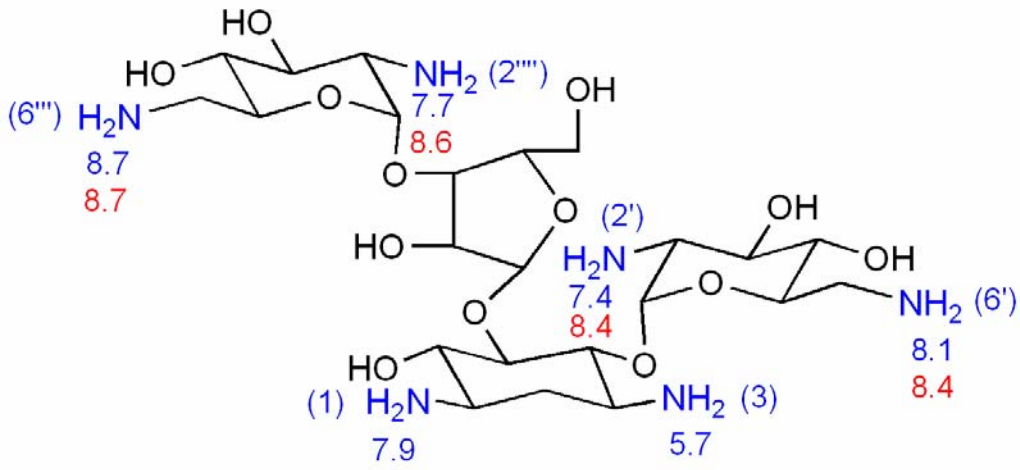

Figure 1. Structure of neomycin B. Amino groups are shown with their numbering indicated in parantheses. The pK_a values of the amino groups in free neomycin (*1*) and in the neomycin–APH complex (this work) are shown in blue and red, respectively.

Materials and Methods

D_2O (99.9%) was from Wilmad LabGlass (Buena, NJ), and ^{15}N-enriched (98%) NH_4Cl was from Cambridge Isotope Laboratories (Andover, MA).

Protein Purification. Purification of APH was described previously (*2*) with the modifications described by Özen and Serpersu (*3*). Purified APH was concentrated using Millipore (Billerica, MA) ultrafiltration membranes and stored at –80 °C. Care was taken to ensure that APH remained as a monomeric protein at all times, and the monomeric state of the enzyme was confirmed by HPLC. The reason for taking these precautions is that APH is known to form dimers via two intermolecular disulfide bonds (*2*), and as shown below, the aminoglycoside binding to the dimer is significantly different from its binding to the monomeric enzyme. We have shown that the monomeric enzyme binds the aminoglycosides with a 1:1 stoichiometry (*3*). However, as shown in Figure 2, our experiments with a largely dimeric enzyme (>90%) demonstrated that one of the monomers has a more than 3 orders of magnitude weakened affinity to aminoglycosides and only tight-binding aminoglycosides, such as neomycin, can populate this low-affinity site. Kanamycin binds half-stoichiometrically under similar conditions. A similar half-stoichiometric binding of aminoglycosides to aminoglycoside acetyltransferase(6′)-Iy (AAC) was also observed with the dimeric enzyme (*4*). Therefore, all experiments described in this paper were performed with enzyme preparations that were confirmed to be in the monomeric state.

Production and Purification of ^{15}N-Enriched Neomycin B. Streptomyces fradiae was obtained from the American Type Culture Collection (Manassas, VA), and the cells

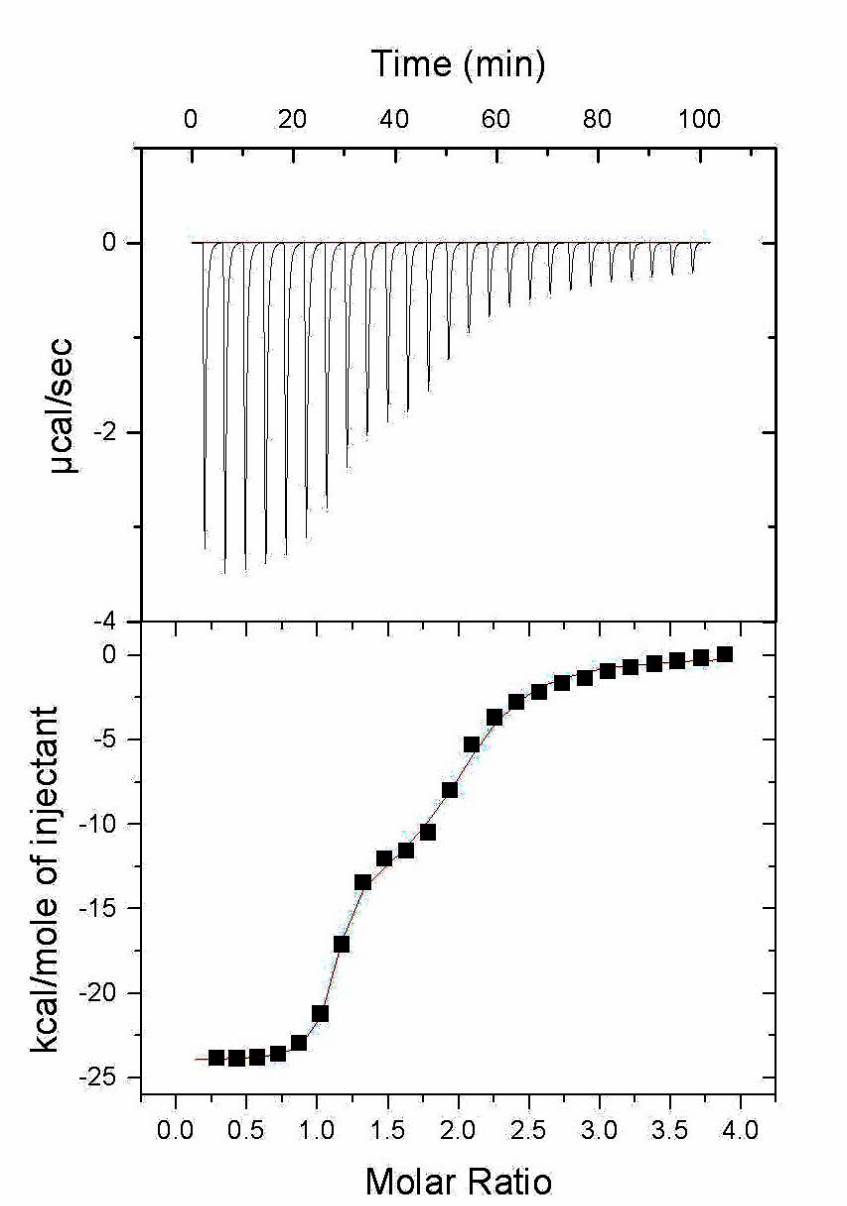

Figure 2. Titration of dimeric APH with neomycin. The thermogram (upper panel) is shown with the fitted data (lower panel), which yields association constants of 1.13 ± 0.37 x 10^8 and 5.9 ± 0.9 x 10^5 M^{-1} for neomycin binding to the first and second binding sites, respectively.

were grown in ISP 4 medium supplemented with $^{15}NH_4Cl$ as the sole nitrogen source in a New Brunswick (Edison, NJ) BioFlo 110 fermentor. The cells were grown at 28 °C for 7 days. Following centrifugation, neomycin was isolated from the supernatant by a method similar to those used for the isolation and purification of kanamycin A (*5*) and ribostamycin (*6*); the supernatant was concentrated and loaded into an IRC-50 weak cation exchange column. HCl (1.0 M) was used for elution, and fractions containing neomycin were combined. Following pH adjustment to 7.0, the sample was concentrated to dryness and treated with methanol/acetone precipitation steps. Desiccated powder was dissolved in 10% methanol and loaded into a C18 HPLC column for further purification using 10% methanol as the mobile phase. The product and its purity were verified by NMR spectroscopy (Figure A in the Appendix) and enzymatic assays.

^{15}N NMR Spectroscopy of Aminoglycosides. ^{15}N-neomycin was diluted from a stock solution to a Shigemi tube (Allison Park, PA) in a total volume of 275 μL at a concentration of 0.5 mM in 90:10 (v/v) H_2O/D_2O. Due to the limited availability of ^{15}N-neomycin and the requirement of a high enzyme-to-neomycin ratio, we initially tried indirect detection by $^{15}N–^{1}H$ heteronuclear single-quantum correlation (HSQC) experiments to achieve higher sensitivity. However, the results were not satisfactory, and therefore, 1D direct detection ^{15}N NMR spectroscopy was used. One-dimensional, ^{1}H-decoupled ^{15}N NMR spectra were recorded as a function of pH for the free and enzyme-bound neomycin at 60.78 MHz on a Varian Inova 600 MHz spectrometer at 25 °C. Although not very high, the S/N ratio was sufficient to detect even crossovers of nitrogen signals in these experiments (Figure 3). When present, APH was ~0.55 mM to ensure that more than 95% of the neomycin was bound to the enzyme except at pH > 9.0, where the

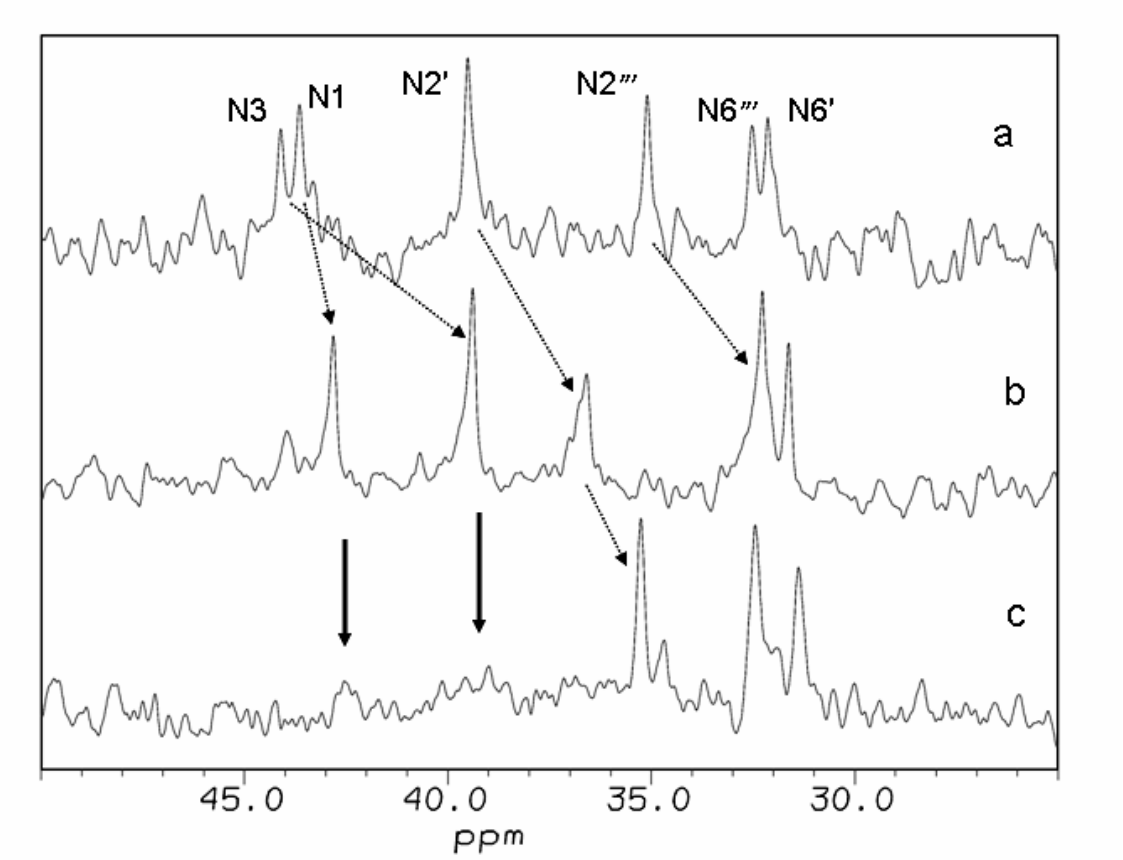

Figure 3. ^{15}N NMR spectrum of 0.5 mM free ^{15}N-neomycin at pH 4.63 (a), at pH 6.80 (b), and at pH 6.73 in the presence of 0.55 mM APH (c). The resonance assignments shown at the top are based on the earlier work by Botto and Coxon (*1*).

occupancy was ~80. Acquisition parameters included a spectral width of 6000 Hz, a 45° pulse length of 20 μs, and a delay of 0.5 s between scans. A total of 8–16K data points of 20000–80000 FIDs were collected. Before Fourier transformation, 10 Hz line broadening was applied. All ^{15}N chemical shifts are referenced to $^{15}NH_4Cl$. The $^{15}NH_4Cl$ (5% enriched) solution was 0.1 M and was prepared in 90:10 (v/v) H_2O/D_2O. The pK_a values of the amino groups of neomycin were determined by fitting the data, plotted as parts per million vs pH, to a nonlinear regression fit using the GraphPad Prism, version 3.02, for Windows, GraphPad Software (San Diego, CA).

Isothermal Titration Calorimetry (ITC) Experiments. A VP-ITC microcalorimeter from Microcal, Inc. (Northampton, MA) was used to conduct the calorimetry experiments. The experimental temperature was 24 °C. A triple-buffer system composed of 25 mM MES, 25 mM HEPES, and 25 mM BICINE was used in the experiments where the binding affinity of aminoglycosides to the enzyme was determined as a function of pH. A single buffer system of 50 mM ACES, PIPES, TRIS, HEPES, BICINE, or TAPS was used for the determination of proton uptake by enzyme–aminoglycoside complexes at different pH values. In all experiments, the final potassium ion concentration was fixed to 100 mM using KCl. Each series of ITC experiments were performed with the same batch of APH that was extensively dialyzed against the ITC buffer, and ligand solutions were prepared in the final dialysate. As indicated above, freshly added DTT was always present in enzyme solutions to prevent dimerization. A 50 μM enzyme solution is titrated with 0.5 mM neomycin under different conditions. Protein and ligand solutions were degassed under vacuum for 10 min before being loaded into the calorimeter cell and syringe. Titrations consisted of 29 injections programmed as

10 μL per injection and separated by 240 s. The cell stirring speed was 300 rpm. The binding constant (K_b) and enthalpy change (ΔH) were obtained by nonlinear least-squares fitting of experimental data using a single-site binding model of the Origin software package (version 5.0). The *C*-value, a parameter obtained by the multiplication of the association constant (K_b) and the total concentration of ligand binding sites (*7*), was within the range of 1–200 in all experiments where reliable determination of the affinity constant is possible. (Abbreviations: MES, 2-morpholinoethanesulfonic acid; HEPES, 4-(2-hydroxyethyl)piperazine-1-ethanesulfonic acid; BICINE, *N*,*N*-bis(2-hydroxyethyl) glycine; ACES, *N*-(2-acetamido)-2-aminoethanesulfonic acid; PIPES, 1,4-piperazinediethanesulfonic acid; TRIS, 2-amino-2-(hydroxymethyl)-1,3-propanediol; TAPS, [(2-hydroxy-1,1-bis(hydroxymethyl)ethyl)amino]-1-propanesulfonic acid; DTT, dithiothreitol.)

Results and Discussion

We employed a combination of NMR and ITC to investigate the role of ionizable groups and proton linkage in neomycin binding to APH. ITC was used to determine the net contribution of ionizable groups to the global thermodynamic properties of the binary enzyme–aminoglycoside complex,while NMR spectroscopy was used to identify changes in the pK_a values of amino groups on the enzyme-bound antibiotic neomycin to determine their individual contributions to the thermodynamics of the APH–neomycin complex.

NMR Studies of Free and Enzyme-Bound Neomycin. Studies of aminoglycosides by ^{15}N NMR have been limited to the use of free aminoglycosides because a high

concentration is required for detection and ^{15}N NMR studies of target-bound aminoglycosides are simply not feasible. Therefore, to date, the pK_a values of amino functions are determined only for free aminoglycosides (*1, 8–11*). In this work, we report the first determination of pK_a values in a target-bound aminoglycoside antibiotic by using uniformly enriched ^{15}N-neomycin, which was prepared from cultures of *S. fradiae* grown in ^{15}N-enriched media as described in the Materials and Methods.

To determine the effects of binding on each amino group of neomycin, we acquired NMR spectra as a function of pH using ^{15}N-enriched neomycin in the absence and presence of APH (Figure 3). Our ^{15}N NMR spectra matched earlier data acquired with isotopically normal neomycin (*1*), and therefore, previously made resonance assignments were applied to our spectra acquired with ^{15}N-neomycin. When present, the enzyme concentration was above the neomycin concentration such that more than 95% of the neomycin was in the binary enzyme–neomycin complex except at very high pH (>9.1, where ~20% of the neomycin was free). The determined pK_a values of the amino groups in free neomycin agreed with the earlier work of Botto and Coxon (*1*) performed with isotopically normal neomycin in the absence of sulfate (sulfate is present in commercial preparations of aminoglycosides and, if not removed, alters the pK_a values of the amino groups significantly).

Addition of enzyme to the neomycin solution showed that resonances of N1 and N3 were significantly broadened while N2′ was shifted upfield (Figure 3). Broadening of N1 and N3 indicates that exchange rates are at an intermediary stage with these amino groups in the enzyme-bound neomycin, which precluded determination of their pK_a values. These observations are consistent with these three nitrogens being part of a

"recognition motif" that adopts the same conformation when bound to enzymes or RNA (*10, 12, 13*). Also, APH shows a strong preference for the aminoglycosides with $-NH_2$ at the 2′-position over those with a –OH (*3*), which is consistent with the observed upfield shift of this resonance upon binding to the enzyme.

Chemical shifts of the four nitrogen signals representing the 2′-, 2‴-, 6‴-, and 6′-NH_2 groups were followed with varying pH. The change in their chemical shift as a function of pH is shown in Figure 4. There was also a general broadening of these signals between pH values of ~8.7 and 9.1, and no reliable data points were obtained within this range for the enzyme–neomycin complex. Better defined end points of titration, however, allowed curve fitting to be applied to determine pK_a values. Therefore, the determined pK_a values for these groups should be considered approximate. When there was an overlap, the titration curves were constructed to conform with the expected shifts for different nitrogens (*1*) to yield a smooth sigmoidal curve. The pK_a values of free and enzyme-bound neomycin are given in Table 1. The data shown in Figure 4, however, still clearly demonstrates significant shifts in the pK_a values of the enzyme-bound neomycin; thus, the small uncertainty in the pK_a values of the enzyme-bound neomycin does not alter the conclusions of this work. To the best of our knowledge, these data represent the first pK_a determination of a target-bound aminoglycoside antibiotic.

As shown in Figure 4, N2′ and N2″ amino groups show the largest shifts and change their pK_a values by about 1 pK_a unit. 6′-NH_2 shows approximately 0.3 unit upshift in its pK_a, and the N6‴ amino group experiences no change in its pK_a. Examination of the crystal structure of the APH–MgADP–neomycin complex (*14*) (Figure 5) shows that 6‴-

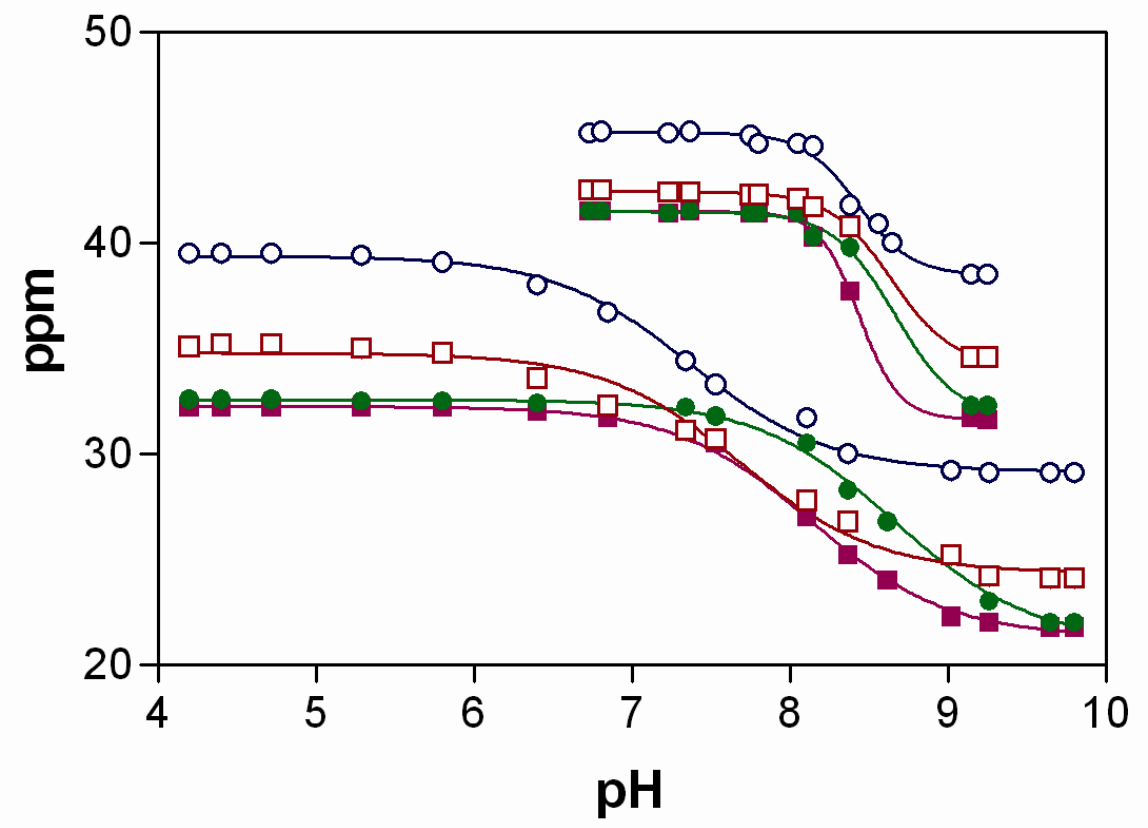

Figure 4. ^{15}N chemical shift titration curves for free (lower curves) and enzyme-bound neomycin (upper curves, which are moved by 10 ppm up for clarity). N2′ (○), N2‴ (□), N6′ (■), and N6‴ (●).

Table 1. pK_a Values of the Amino Groups in Free and Enzyme-Bound Neomycin[a]

	N1	N3	N2′	N6′	N2″′	N6″′
free neomycin	7.9 ± 0.05	5.7 ± 0.06	7.4 ± 0.04	8.1 ± 0.02	7.7 ± 0.07	8.7 ± 0.04
APH–neomycin	ND	ND	8.4 ± 0.03	8.4 ± 0.02	8.6 ± 0.04	8.7 ± 0.1

[a]Uncertainties represent curve fitting errors.

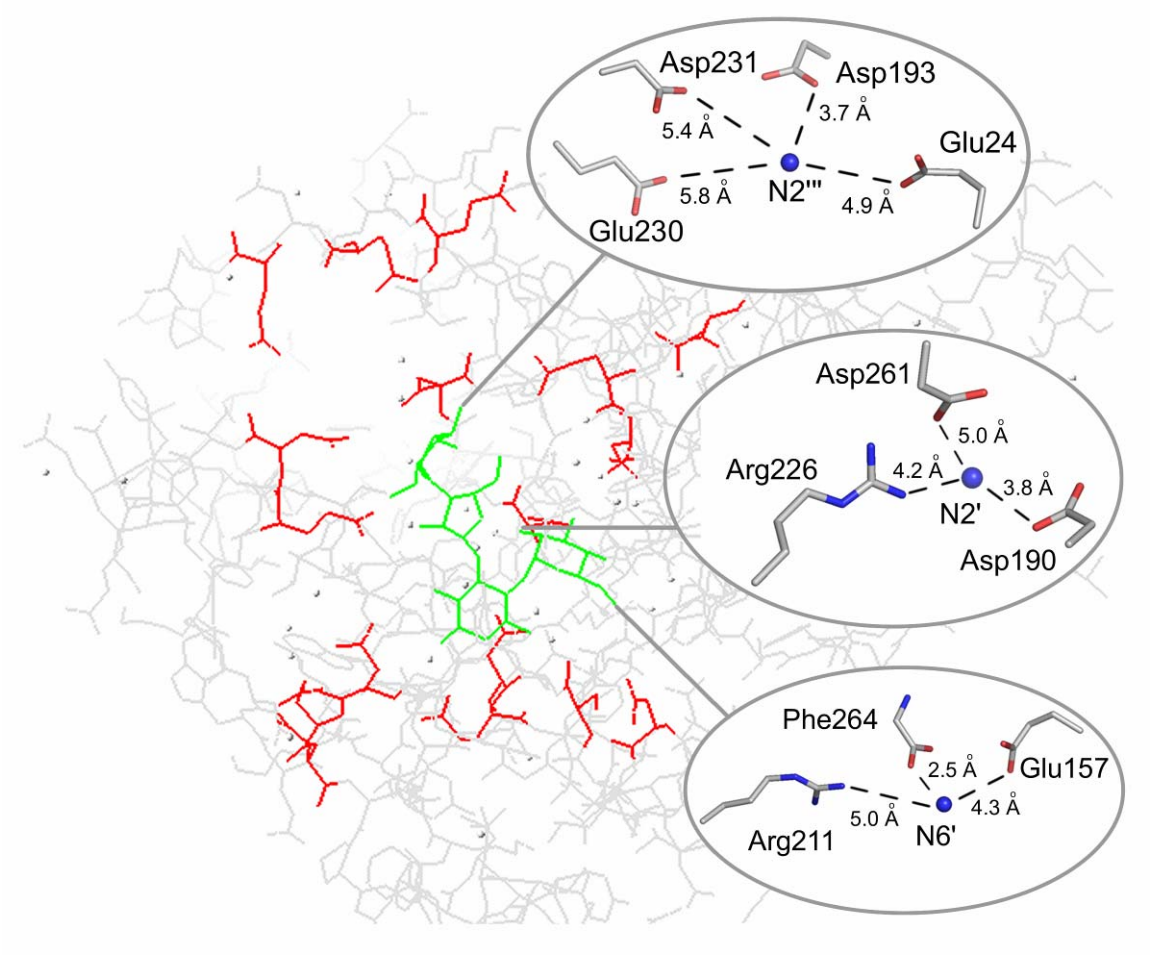

Figure 5. Crystal structure of APH–MgADP–neomycin (*14*). Bound neomycin (green) is surrounded by a large number of acidic residues (red). The immediate environment of the three amino groups that show an upshifted pK_a are shown in expanded views. This figure was created by using Pymol[26] and DeepView[27] software.

NH_2 is exposed to solvent and the nearest carboxyl group (E230) is more than 4.5 Å away. Thus, no change in its pK_a is consistent with the orientation of enzyme-bound neomycin. The N2′ and N2‴ amino groups showed the largest shifts. The N2′ amino is likely to form a hydrogen bond with D190; similarly, D193 is within a H-bond distance of N2‴. Thus, the shifts observed are consistent with the crystal structure of the enzyme–MgADP–neomycin complex (*14*). The 6′-amino group, on the other hand, is within 2.5 Å of the carboxyl group of the Phe 264, which is at the C-terminus. E157 is also ~4.3 Å away from the 6′-amino group, yet the 6′-NH_2 experiences only a shift of ~0.3 pK_a unit. This is not consistent with the crystal structure, which suggests that either the dynamic properties or the conformation of the binary enzyme–neomycin complex is different around this amino group compared to its environment in the enzyme–MgADP–neomycin complex.

Of the two amino groups whose pK_a values could not be determined, N1 is within 3 Å of E262 and less than 4 Å away from E160. Similarly, N3 is within a 3 Å distance from E157 and ~4.2 Å from D261. It is very likely that these groups experience significant shifts. Also, their proximity to more than one carboxyl side chain is consistent with their exchange properties. These observations show that at least three amino groups of neomycin experience an upshift in pK_a, which causes further protonation in these groups upon binding to the enzyme. This number does not include N1 and N3, both of which are expected to have a shifted pK_a. On the basis of these structural considerations, one would think that the increased protonation of the amino groups in neomycin should, in principle, increase the affinity of the antibiotic to the enzyme. However, as will be described later, ITC experiments showed that the binding of neomycin to APH is affected

by additional interactions, some of which may still dominate at low pH and reduce the affinity of neomycin to APH despite a highly charged state of this antibiotic.

We note that the NMR data acquired with the binary enzyme–neomycin data are evaluated using the structure of the quaternary enzyme–Mg^{2+}–ADP–neomycin complex due to unavailability of a structure for the binary enzyme–aminoglycoside complex. The selection of the binary complex for these studies is, however, still justified. First, when a metal–nucleotide complex is added to APH or the APH–aminoglycoside complex, no or very small changes are observed in the ^{15}N-^{1}H HSQC spectra. Contrary to this, addition of an aminoglycoside to the enzyme or enzyme–metal–nucleotide complex alters both spectra significantly and yields almost identical spectra for both complexes (*15*). These observations suggest that the environment of bound neomycin is similar in the binary and the quaternary complexes; thus, the conclusions of this work may largely be applicable to both complexes. These observations are fortuitous, but the main reason for the selection of the binary system is more significant and involves difficulties of data interpretation. ITC experiments described in the following sections are interpreted with the help of NMR data to understand the contributions of the microscopic protonation event to the calorimetric parameters. This requires that the calorimetrically observed parameters should reflect the behavior of the complex of interest only. While the thermodynamics of a binary system can be described by a single equilibrium, a ternary system can be described by six interdependent equilibria (*16, 17*), and a complete description of a quaternary system such as APH, Mg^{2+}, nucleotide, and aminoglycoside requires more than a dozen equilibria (in reality it is even more complicated than this because there two bound Mg^{2+} ions can be seen in the crystal structures (*14*)). Thus, at each titration point,

the concentrations of various species will change and all dissociations and associations will contribute to the observed heat of reaction. Therefore, it would be practically impossible to determine the effects of pH on the relevant equilibrium alone (binding of neomycin to the enzyme–Mg^{2+}–nucleotide complex), since all equilibria may be affected differentially as the pH is varied. Thus, attribution of the effects of pH or any other variable to the relevant complex (enzyme–metal–ATP–aminoglycoside) can be very difficult.

Calorimetric Studies. Two different calorimetric approaches were used to determine binding-linked protonation/deprotonation and the effect of pH on the formation of the binary enzyme–neomycin complex. The first method involves determination of the observed enthalpy change (ΔH_{obs}) upon ligand (aminoglycoside) binding to the enzyme in buffers with different ionization enthalpies (ΔH_{ion}) to derive the intrinsic enthalpy change (ΔH_{int}) and the net number of binding-coupled proton exchanges (Δn). In the presence of binding-linked protonation, the observed enthalpy (ΔH_{obsd}) includes contributions from various sources according to the equation

$$\Delta H_{obsd} = \Delta H_{int} + \Delta n[\alpha\Delta H_{ion} + (1 - \alpha)\Delta H_{enz}] + \Delta H_{bind} \quad (18)$$

in which ΔH_{int} is the intrinsic enthalpy of binding, Δn represents the net proton transfer, ΔH_{obsd} denotes the observed binding enthalpy of complex formation in a buffer, ΔHion describes the heat of ionization of the buffer, the term $\Delta n[\alpha\Delta H_{ion} + (1 - \alpha)\Delta H_{enz}]$ represents the heat of ionization of groups from the ionization of the buffer and the protein to maintain the pH, where α represents the fraction of protonation contributed by the buffer (*18*), and ΔH_{bind} represents the heat of binding of the buffer to the enzyme. In the presence of high salt (i.e., 100 mM KCl), ΔH_{bind} is assumed to be zero and the

contribution from the ionization of amino acids remains the same at a given pH. Thus, by performing experiments in buffers with different heats of ionization, one can easily determine ΔH_{int} and Δn. However, note that ΔH_{int} still includes the heat of ionization of groups contributing to Δn (i.e., $\Delta H_{int} = (\Delta H_{int} + \Delta H_{functional\ groups}\Delta n)$ which would represent the true ΔH_{int} only when $\Delta n = 0$). For the buffers used in this work, a net proton uptake by the enzyme–ligand complex yields a positive Δn.

Binding-Linked Protonation. Binding-linked protonation was observed in the formation of the binary APH–neomycin complex. Values of ΔH_{int} and Δn showed a strong dependence on pH as shown in Table 2. An interesting observation was made that there appeared to be no net binding-linked protonation or a small deprotonation occurs at pH 6.7 ($\Delta n \approx 0$). This is usually taken as an indication that the determined ΔH_{int} under these conditions may be used as the true ΔH_{int}, which is free of contributions of ΔH_{ion} of the ligand and/or enzyme groups. This is somewhat surprising because one would expect the pK_a of N3 to upshift upon binding to the enzyme due to its proximity to the carboxyl groups (Figure 5). This would alone contribute to the observed Δn by ~+0.4 at this pH. In addition, shifts observed in the pK_a values of N2′ and N2‴ cause a contribution of an additional ~0.24 from these groups, making the overall expected contribution to the observed Δn to be >0.6. Thus, it is likely that deprotonation of another group may compensate for the combined protonation of N3, N2′, and N2‴, yielding an overall $\Delta n \leq 0$. Analysis of the data in Table 2, as described below, lends further support to the suggestion that other protonation/deprotonation reactions also accompany the formation of the enzyme–neomycin complex.

Table 2. pH-Dependent Intrinsic Enthalpy Change (ΔH_{int}) and Net Number of Binding-Coupled Proton Transfers (Δn) for the Neomycin–APH Complex

pH	buffer	ΔH_{ion}[a] (kcal/mol)	ΔH_{obsd}[b] (kcal/mol)	ΔH_{int} (kcal/mol)	Δn
6.7	ACES	7.5	–16.8 ± 1.7	–15.7 ± 2.0	–0.1 ± 0.0
6.7	PIPES	2.7	–16.1 ± 1.6		
7.6	TRIS	11.4	–9.3 ± 0.9	–26.5 ± 3.4	1.5 ± 0.3
7.6	HEPES	5.0	–18.9 ± 1.9		
8.5	BICINE	6.5	–21.9 ± 2.2	–38.0 ± 4.9	2.5 ± 0.4
8.5	TAPS	9.0	–13.3 ± 1.3		

[a]Taken from Fukada and Takahashi, 1998. [b]Determined at 297 K. Uncertainties reflect combined fitting errors and standard error of mean for the replicates.

If one assumes that ΔH_{int} determined at pH 6.7 is the true intrinsic enthalpy, then one can estimate ΔH_{ion} of groups involved in protonation, which may then yield clues to the nature of these groups. The heat of formation (ΔH_{int}) of the binary APH–neomycin complex becomes more negative with increasing pH. When ΔH_{int}, determined at the regime where $\Delta n = 0$, is subtracted from values obtained at regimes where $\Delta n \neq 0$ and the result divided by Δn, the contribution due to ΔH_{ion} of group(s) involved in binding-linked protonation (groups with a shifted pK_a) may be revealed. Such a calculation yields ΔH_{ion} of –7.2 and –8.9 kcal/mol for the formation of the APH–neomycin complex at pH 7.6 and 8.5, respectively. These values are somewhat lower than ΔH_{ion} of the amino groups, which is about 9–10 kcal/mol (*19*). Assuming that the contribution of other factors such as cooperativity of hydrogen bonds to ΔH_{int} remains unaltered, these data suggest that several functional groups may be undergoing protonation/deprotonation reactions. Therefore, the observed ΔH_{ion} represents an "average" value and precludes identification of the types of functional groups with altered pK_a values. These data also show that the value observed for ΔH_{ion} at higher pH contains more contributions from the amino groups since its value is closer to ΔH_{ion} of the amino groups (*19*). This appears to be a trend in aminoglycoside–enzyme interactions. Even a larger increase in ΔH_{ion} (from –6.4 to –10.8 kcal/mol) was observed with increasing pH in the aminoglycoside nucleotidyltransferase(2″)-Ia–neomycin complex (Wright and Serpersu, unpublished data), which suggests that, at high pH, protonation of the amino groups is likely to be the major contributor to ΔH_{ion} in that complex as well.

We also attempted to dissect contributions of individual amino groups of neomycin to the observed thermodynamic parameters. A simple calculation shows that

the protonation of the N2′, N2‴, and N6′ amino functions should contribute to the observed Δn by about 0.97 and 1.0 at pH 7.6 and 8.5, respectively. If the observed Δn were solely due to the protonation of neomycin, then this would leave N3 and N1 as the only amino groups to make up the rest of the observed Δn values. However, no combination of pK_a values can be assigned to these groups that would add up to Δn to match the observed values at both pH values. This, again, strongly suggests that protonation/deprotonation of other groups must contribute to the observed thermodynamic parameters. The active site of APH has only Asp, Glu, and Arg side chains as functional groups (Figure 5), none of which are normally expected to be involved in protonation/deprotonation in the pH regime studied. The likely functional group to contribute in this pH regime may be the imidazole side chain. However, the nearest histidine residue to any part of neomycin is ~9 Å away and is shielded from neomycin by other residues. Thus, these observations also suggest propagation of effects to remote sites upon binding of aminoglycoside to the enzyme. Such remote effects have been detected with other proteins (*20*).

The combined contribution of N2′, N2‴, and N6′ would be ~10 kcal/mol at pH 7.6. Since they also account for a contribution of ~1 to Δn, this would leave only 0.8 kcal/mol for an additional Δn of ~0.5, which is too small for any heat of ionization reaction except for carboxyl groups. This would imply that either there is no change in the pK_a values of N1 and N3, which is very unlikely, or compensatory ionization by other groups contributes to the observed enthalpy. Furthermore, the same calculation for the data obtained at pH 8.5 yields ~12.3 kcal/mol for the additional Δn of ~1.5, leaving ~8.2 kcal/mol, a value much closer to the heat of ionization of the amino groups. In this case,

it is possible that, at pH 8.5, almost all of the heat of ionization can be attributed to the protonation of five amino groups in neomycin. Thus, experiments performed at two different pH values suggest that all protonation may occur on the ligand at high pH; however, at pH 7.6, other functional groups also undergo protonation/deprotonation reactions.

Enzyme–Aminoglycoside Association as a Function of pH. The second calorimetric method involves determination of K_b for the formation of binary enzyme–aminoglycoside complexes as a function of pH. The effect of the pH on K_b for the formation of the APH–neomycin complex was investigated by ITC. A pH range of 6.8–9.1 was used in a triple-buffer system.

The dramatic effect of the pH on K_b is shown in Figure 6 in representative ITC titrations. The affinity of neomycin to the enzyme was reduced at high pH. However, K_b does not necessarily correlate with the fractional charge on the aminoglycosides. As shown in Figure 7, the affinity (K_b) of neomycin to the enzyme was increased first with increasing pH up to pH 8.1,showed a plateau between pH 8.1 and 8.4, and then decreased sharply above pH 8.4. The difference between the highest and lowest K_b is more than 60-fold in the APH–neomycin complex. The increase in affinity appears to correlate with Δn and inversely correlate with the total fraction of $-NH_3^+$ ions in neomycin in the pH range of 6.8–8.4. The sum (Δn + [$-NH_3^+$]), however, remains essentially unchanged between pH 6.8 and pH 8.4, and yet K_b increases by a factor of ~6.5-fold within the same pH range. An increase in affinity with increasing pH suggests that deprotonation of a group or more is contributing favorably to the binding of neomycin to APH. This deprotonation is most likely to be from a functional group(s) in the enzyme.

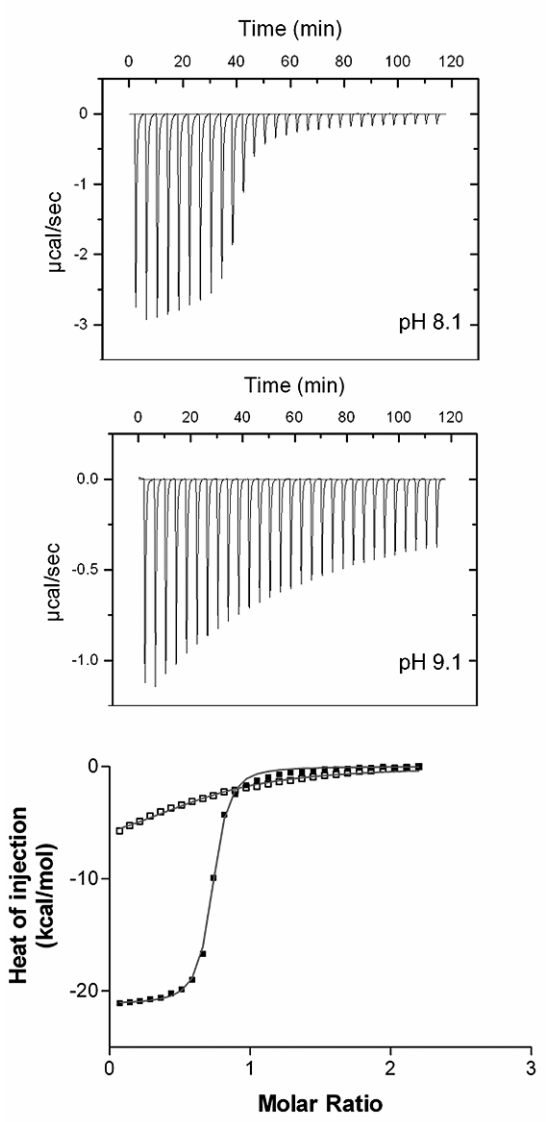

Figure 6. Titration isotherms of neomycin to APH at pH 8.1 (■) and pH 9.1 (□). Raw data (thermal power) are given in the two upper panels. The bottom panels show the heat of injection, which is obtained by integration of the thermal power, plotted against the molar ratio of ligand to enzyme. Nonlinear curve fitting of the binding data is shown with a solid line. The observed binding constants (K_b) obtained from the fits of these and other pH experiments are given in Table 2.

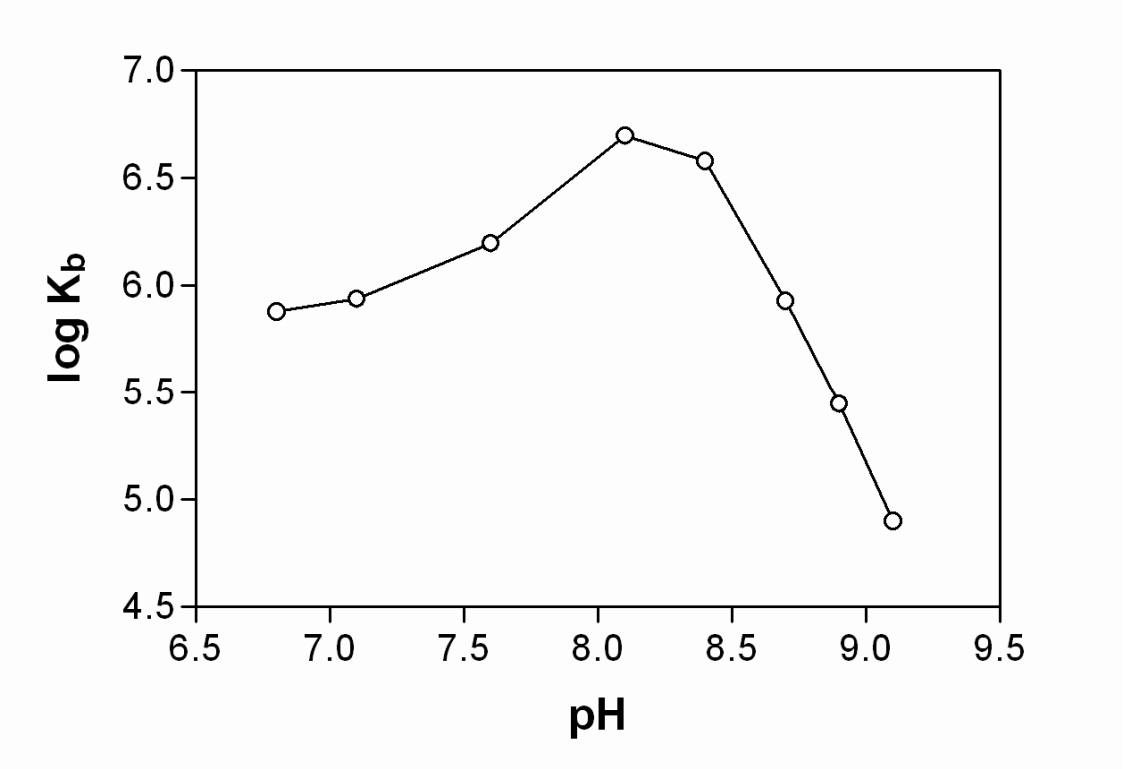

Figure 7. Association constant (K_b) for the binary APH–neomycin complex as a function of pH.

The increase in K_b of the APH–neomycin complex as the pH is raised from 6.8 to 8.4 is not easy to explain. Using the determined pK_a values of four of the six amino groups in enzyme-bound neomycin, one can now determine the protonation state of the N2′, N2‴, N6′, and N6″ amino groups. At pH 6.8, these groups are >95% protonated. Their protonation is reduced to ~70% at pH 8.1. Thus, the net positive charge on neomycin experiences a decrease in this pH range, yet it has an increased affinity to the enzyme. It is not clear how the decrease in charge would increase the affinity of neomycin to APH, because almost all amino groups of enzyme-bound neomycin are near carboxyl functions in the active site. The N1 amino and the 2′-amino are the only groups that are near a positively charged enzyme functional group (R226). Early kinetic studies showed that an amino group at N1 and an amino or hydroxyl at the 2′ position is needed for a lower K_m (*21*). Binding studies showed that aminoglycosides with an amino function at the 2′ position bind to APH and other aminoglycoside-modifying enzymes tighter than those with a hydroxy at this position and show significantly different thermodynamic properties (*3, 22*). There are no enzyme functional groups that are good candidates in the active site of APH to undergo protonation/deprotonation in this pH range. Also, the only basic side chain belongs to R226, which, normally, has a too high pK_a to be affected in the pH range studied for binding. This leaves us with an option that either deprotonation of an enzyme side chain remote from the active site is increasing K_b via conformational changes in the enzyme, or as shown in Figure 5, the N2′ amino group of neomycin, despite its higher shifted pK_a, may still contribute favorably upon deprotonation because it is the closest amino group to R226 (~4.2 Å away). However, it is also near two carboxyl functions, D190 and D261. Thus, the upshift in its pK_a and its

contribution to K_b may be determined by the interplay of two opposing effects; while the positively charged N2′ amino interacts favorably with carboxyls, its interaction with R226, on the other hand, may oppose this. In this pH range, the charge on the N2′ amino group is reduced by 30% at pH 8.1 starting from a fully charged (>98%) state at pH 6.8. Thus, as the pH is raised, the unfavorable interaction between this group and R226 will be reduced. Another amino group that may also contribute to this is the N1 amino group, which is ~4.4 Å away from R226. This is, however, less likely because the pK_a of N1 is already 7.9 in free neomycin and it is likely to be upshifted significantly upon binding because it is near two carboxyl groups. If this is the case, then its bound pK_a may simply be too high to cause a significant deprotonation of N1 in the pH range of 6.8–8.1. In light of this, the observed effect of the pH on K_b may still reflect, in part, deprotonation of the 2′-amino group in neomycin.

Conclusions

In this work, we determined the pK_a values of amino groups for an aminoglycoside bound to one of its target molecules, an enzyme causing resistance to these antibiotics. The data permitted us to determine contributions of selected amino groups of the ligand to the global thermodynamic properties of the enzyme–ligand complex. Studies described in this paper show that binding of aminoglycoside antibiotics to APH involves a complex pattern of protonation and deprotonation of substrate amino groups and functional groups of the enzyme. Contributions from different groups at different pH values further complicate data analysis. These findings highlight problems associated with attribution of thermodynamic parameters to specific sites even in a simple

binary enzyme–ligand complex and underline the importance of the determination of thermodynamic parameters of a system under different conditions before attributing the observed changes in global thermodynamic parameters to specific residues/sites. These studies also showed that, along with structural studies, studies to determine dynamic and thermodynamic properties of enzyme–aminoglycoside complexes are necessary to understand the factors contributing to the formation of enzyme–aminoglycoside complexes.

Overall, results described in this paper showed that the thermodynamics of the binary enzyme–aminoglycoside complexes are strongly dependent on environmental factors such as the pH and its effect on the ionizable groups of aminoglycosides. Formation of the binary aminoglycoside–APH complex is coupled to a net protonation of several amino groups on the ligand. However, global parameters such as Δn, determined by thermodynamic studies, can sometimes be misleading. In our case, a net protonation was indicated by the positive sign of Δn upon binding of neomycin to APH, but other studies clearly showed that binding was also accompanied by deprotonation of other groups, which was masked in the global parameter Δn. In conclusion, a combination of NMR and calorimetric studies permitted dissection of the thermodynamic properties of an enzyme–aminoglycoside complex, and the contributions of individual sites on the ligand to the formation of the enzyme–ligand complex were determined.

Acknowledgements

This research was supported by a Grant from the National Science Foundation (MCB 01110741 to E.H.S.) and the Center of Excellence for Structural Biology at The University of Tennessee.

List of References

References

1. Botto, R. E. a. C., B., *Journal of the American Chemical Society* **1983,** 105, 1021-1028.
2. McKay, G., A., Thompson, P. R., and Wright, G. D., *Biochemistry* **1994,** 33, 6936-6944.
3. Ozen, C.; Serpersu, E. H., *Biochemistry* **2004,** 43, (46), 14667-14675.
4. Hedge, S. S., Dam, T. K., Brewer, C. F., Blanchard, J. S., *Biochemistry* **2002,** 41, 7519-7527.
5. Umezawa, H.; Ueda, M.; Maeda, K.; Yagishita, K.; Kondo, S.; Okami, Y.; Utahara, R.; Osato, Y.; Nitta, K.; Takeuchi, T., *J. Antibiotics, Ser. A* **1957,** 10, (5), 181-8.
6. Shomura, T.; Ezaki, N.; Tsuruoka, T.; Niwa, T.; Akita, E.; Niida, T., *J. Antibiot.* **1970,** 23, (3), 155-&.
7. Wiseman, T.; Williston, S.; Brandts, J. F.; Lin, L. N., *Anal. Biochem.* **1989,** 179, (1), 131-7.
8. Cox, J. R.; Serpersu, E. H., *Biochemistry* **1997,** 36, (9), 2353-2359.
9. Dorman, D. E., Paschal, J. W., and Merkel, K. E., *J. Am. Chem. Soc.* **1976,** 98, 6885-6888.
10. Cox, J. R.; Ekman, D. R.; DiGiammarino, E. L.; Akal-Strader, A.; Serpersu, E. H., *Cell Biochem. Biophys.* **2000,** 33, (3), 297-308.
11. Barbieri, C. M. a. P., D. S., *Biophys. J.* **2006,** 90, 1338-1349.
12. Serpersu, E. H.; Cox, J. R.; DiGiammarino, E. L.; Mohler, M. L.; Ekman, D. R.; Akal-Strader, A.; Owston, M., *Cell Biochem. Biophys.* **2000,** 33, (3), 309-321.
13. Owston, M. A.; Serpersu, E. H., *Biochemistry* **2002,** 41, (35), 10764-10770.
14. Fong, D. H.; Berghuis, A. M., *Embo J.* **2002,** 21, (10), 2323-2331.
15. Welch, K. T., Virga, K. G., Brown, C. L., Wright, E., Lee R. E., and Serpersu, E. H., *Bioorg. Med. Chem.* **2005,** *13*, 6252-6263.
16. Serpersu, E. H., Shortle, D., Mildvan, A. S., **1986,** 25, 68-77.
17. Serpersu, E. H., Shortle, D., Mildvan, A. S., *Biochemistry* **1987,** 26, 1289-1300.
18. Atha, D. H. a. A., G. K., *Biochemistry* **1974,** 13, 376-23822.
19. Christensen, T.; Svensson, B.; Sigurskjold, B. W., *Biochemistry* **1999,** 38, (19), 6300-6310.
20. Freire, E., *Proc. Natl. Acad. Sci. USA* **1999,** 96, 10118-10122.
21. McKay, G. A.; Roestamadji, J.; Mobashery, S.; Wright, G. D., *Antimicrobial Agents and Chemotherapy* **1996,** 40, (11), 2648-2650.
22. Wright, E. a. S., E. H., *Biochemistry* **2005,** 44, 11581-11591.

PART IV: SOLVENT REORGANIZATION AND HEAT CAPACITY CHANGE IN AMINOGLYCOSIDE-APH COMPLEXES

Introduction

Water is a component in binding reactions with significant structural and energetic contributions. As the solvent of life, water plays crucial structural and functional roles in biomolecular interactions. Although its complex role is a poorly understood subject, it is well known that water is a reactant in binding reactions with significant energetic contributions (*1-4*). Solvent accessible surfaces of protein and ligand molecules are covered with water molecules (solvation) in their unbound states. With the formation of a binding complex, some of these water molecules are removed from the binding interface and returned to the bulk solvent (desolvation). Some water molecules may be trapped in protein-ligand interface and facilitate hydrogen bond networks. Solvent reorganization refers to these structural changes and has both enthalpic and entropic contributions to the energetics of complexes.

One of the primary methods to evaluate the contribution of solvent to binding energetics is to determine enthalpy change (ΔH) of binding in light and heavy water (*5, 6*) Enthalpy of a hydrogen bond is approximately 10% higher in D_2O because deuterium forms stronger and more localized hydrogen bonds. Due to this difference, displacement of water molecules from apolar surfaces and formation of hydrogen bonds between displaced and bulk solvent molecules will result in an enthalpic difference which is a measure of desolvation ΔH. Calorimetric studies utilizing solvent isotope effect on different biomolecular systems such as protein-carbohydrate, small molecule-small molecule, protein-peptide, and protein-nucleic acid show that ΔH of binding decreases in D_2O. This change is compensated by entropic terms which leave ΔG typically unchanged. According to the conclusion of these studies, 25 to 100% of observed ΔH can

originate from solvent reorganization (*6, 7*).

Heat Capacity Change of Binding Interactions. Constant pressure heat capacity change (ΔCp) is a thermodynamic parameter closely related to solvent reorganization (*4*). In the context of biomolecular interactions, constant pressure heat capacity change is the extent to which binding enthalpy and entropy change with temperature under constant pressure. Analysis of ΔCp can provide insights into the molecular forces driving binding interactions (*8-12*). Since titration calorimetry is the only technique that allows direct determination of heat of reaction, we employed it to determine the change in the binding enthalpies of APH complexes with kanamycin A and neomycin B as a function of temperature. ΔCp for aminoglycoside-APH complexes were calculated using standard equation;

$$\Delta C_{\mathrm{p}} = \frac{\partial \Delta H}{\partial T}$$

Over the short temperature range we studied, ΔCp didn't show significant temperature dependence and therefore partial derivative terms in ΔCp equation were approximated to ΔΔH / ΔT which is equal to the slope of the best-fit lines in ΔH vs temperature plots.

Results reported in this section indicate a significant role played by solvent in aminoglycoside-APH binding. Interestingly, solvent organization seems to be different in the complexes of different classes of aminoglycosides. We report an unusually large negative heat capacity change for APH-aminoglycoside complexes. A break in ΔCp as well as in the temperature-dependent chemical shift patterns of four enzyme residues are

also observed in the APH–kanamycin complex. These residues may represent *solvent reorganization sites* on the enzyme that are away from the ligand binding site.

Materials and Methods

The aminoglycoside phosphotransferase(3')-IIIa (APH) was purified as described in Part II. DTT was purchased from Inalco Spa (Milano,Italy). D2O and ^{15}N-enriched salts were purchased from Cambridge Isotope Laboratories (Andover, MA).

Isothermal Titration Calorimetry (ITC). Calorimetry experiments were conducted using a VP-ITC microcalorimeter from Microcal, Inc. (Northampton, MA). Concentration of APH in calorimetry sample cell was 20 μM. Aminoglycoside concentration in syringe was in the 0.4 to 0.5 mM range. A buffer system composed of 50 mM HEPES, pH 7.2, and 10 mM DTT (freshly added to the enzyme solution and incubated 1 hr at 24ºC before titration) was used in all experiments. Sodium ion concentration was adjusted to 100 mM using NaCl. H_2O/D_2O experiments were also carried out at 24ºC. Uncorrected pH-meter readings were used. In a few control experiments pD was adjusted according to pD = pH + 0.4 and no significant difference in thermodynamic parameters is observed. pH of samples used in measurement of the change in heat capacity experiments were also adjusted at each temperature. Samples were degassed under vacuum for 10 min before loading to cell and syringe of the calorimeter. Each titration experiment was set for 29 injections of 10 μL ligand solution into the sample cell with 240 sec separation. Stirring speed was set to 300 rpm. Origin software package (v0.5) was used for non-linear least squares fitting of binding data to a single site binding model.

Accessible Surface Area Calculations. Solvent accessible surface areas were calculated using NACCESS software (*13*). Water probe size was defined as 1.4 A. Since binary APH-aminoglycoside crystal structures were not available, we used APH-ADP binary complex (*14*) and APH-MgADP-Kan or APH-MgADP-Neo crystal structures (*15*) to approximate the accessible surface area changes upon aminoglycoside binding. ΔASA associated heat capacity changes were calculated using parametrization developed by Murphy and Freire (*16*).

NMR Spectroscopy. NMR spectra were acquired on a 600 MHz Varian INOVA spectrometer equipped with a triple-resonance probe using uniformly ^{15}N-enriched APH. NMR samples contained 250 μM ^{15}N-enriched APH in 50 mM HEPES buffer, pH 7.5, with 350 μM Kanamycin A or 300 μM Neomycin B to ensure at least a 95% saturation of the binding sites. DTT was also present at 10 mM concentration to prevent dimerization of the enzyme. Sensitivity-enhanced ^{1}H–^{15}N HSQC spectra (*17*) with the TROSY option (*18*) were acquired in the phase-sensitive mode using the States-Haberkorn method for quadrature detection in the indirect dimension (*19*). Datasets were obtained with a spectral width of 8012 Hz in the 1H dimension and 2500 Hz in the ^{15}N dimension and 32-64 scans of 2048 real time points for each of 80 t1 increments were recorded. The data were processed using the Felix processing software package (Accelerys, San Diego, CA) and displayed using either NMRview5 or Sparky (T. D. Goddard and D. G. Kneller, SPARKY 3, University of California, San Francisco) software. The ^{15}N dimension was zero-filled to 256 pts, with the sensitivity enhancement option selected on the left half of the spectrum. No baseline correction or other cosmetic procedures were applied.

Results

Calorimetry Experiments with Solvent Isotopic Substitution. To study the effects of solvent on the formation of aminoglycoside-APH complexes, we determined binding parameters in H_2O and D_2O using ITC. Results are reported in Table 1. Difference of enthalpy change ($\Delta\Delta H$) for complexes in H_20 and D_2O is plotted in Figure 1.

As typically observed in carbohydrate-protein interactions (*20, 21*) , kanamycin group of aminoglycosides (kanamycin A, kanamycin B and tobramycin) showed more negative ΔH values in H_2O whereas neomycin class aminoglycosides (neomycin B, paromomycin I and ribostamycin) yielded more negative ΔH values in D_2O.

Heat Capacity Change of Aminoglycoside-APH Complexes. ΔH of kanamycin A and neomycin B binding to APH was investigated as a function of temperature to determine heat capacity change (ΔCp) of respective aminoglycoside-enzyme complexes. Results are summarized in Table 2.

Change in binding enthalpies of both aminoglycosides show strong temperature dependence, yielding large negative ΔCp values which were calculated using linear regression of ΔH vs temperature plots (Figure 2).

Neomycin-APH complex shows a linear change in ΔH as the temperature changes in the range of 18 to 35ºC with a ΔCp of -1.6 kcal/mol·deg. On the other hand, kanamycin binding shows a biphasic behavior with a break at 30ºC. In the range of 18 to 30ºC, ΔCp value for kanamycin-APH complex is -0.7 kcal/mol·deg, which increases 5-fold and becomes -3.8 kcal/mol·deg in 30 to 37ºC range. As shown in enthalpy-entropy compensation (EEC) plots (Figure 3), changing ΔH values with temperature are compensated by entropic contributions. Linear regression of EEC plots yielded slopes of

Table 1. Solvent Isotope Effect on Aminoglycoside-APH Binding Parameters (kcal/mol).

	ΔG		ΔH		$\Delta\Delta H$
	H_2O	D_2O	H_2O	D_2O	
Kanamycin A	-7.3	-7.1	-23.9	-21.6	-2.3
Kanamycin B	-6.9	-7.0	-18.9	-16.1	-2.8
Tobramycin	-6.8	-6.9	-16.7	-13.4	-3.3
Neomycin B	-8.2	-7.5	-17.0	-23.4	6.4
Paromomycin	-9.1	-7.7	-15.3	-18.0	2.7
Ribostamycin	-8.9	-8.3	-15.1	-16.2	1.1

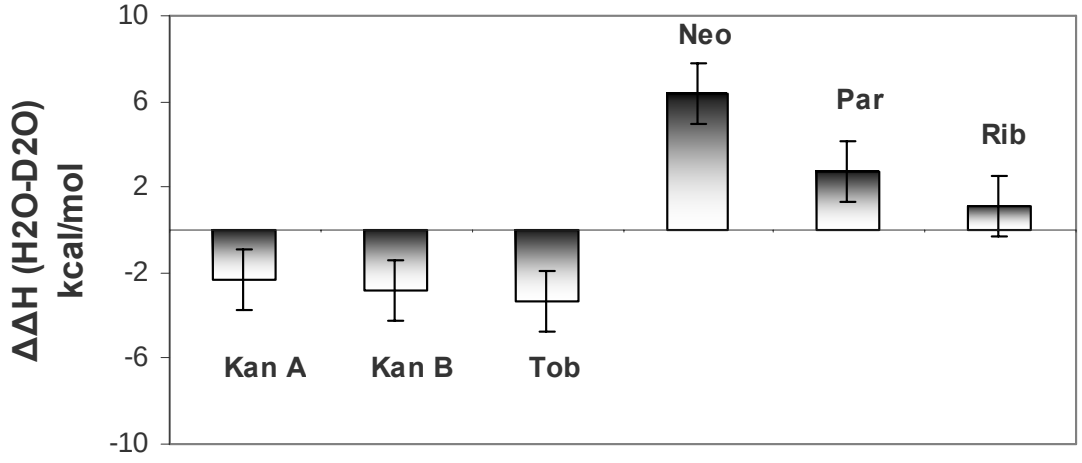

Figure 1. $\Delta H(H_2O) - \Delta H(D_2O)$ ($\Delta\Delta H$) values for kanamycins and neomycins.

Table 2. Thermodynamic data for the complexes of APH with aminoglycosides

	Kanamycin-APH			Neomycin-APH		
Temp (°C)	Δ*H* (kcal/mol)	-TΔ*S* (kcal/mol)	Δ*G* (kcal/mol)	Δ*H* (kcal/mol)	-TΔ*S* (kcal/mol)	Δ*G* (kcal/mol)
18	-13.7	6.2	-7.5	-14.9	6.6	-8.3
21	-14.0	6.4	-7.6	-16.7	8.2	-8.5
24	-18.7	10.8	-7.9	-19.9	11.3	-8.6
27	-19.3	11.3	-8.0	-25.2	16.5	-8.7
30	-21.5	13.3	-8.2	-31.0	22.0	-9.0
32	-26.5	18.2	-8.3	-	-	-
33	-	-	-	-37.3	27.2	-10.1
34	-31.0	22.7	-8.3	-	-	-
35	-	-	-	-41.0	30.4	-10.6
35.5	-37.7	29.4	-8.3	-	-	-
37	-50.2	41.9	-8.3	-	-	-

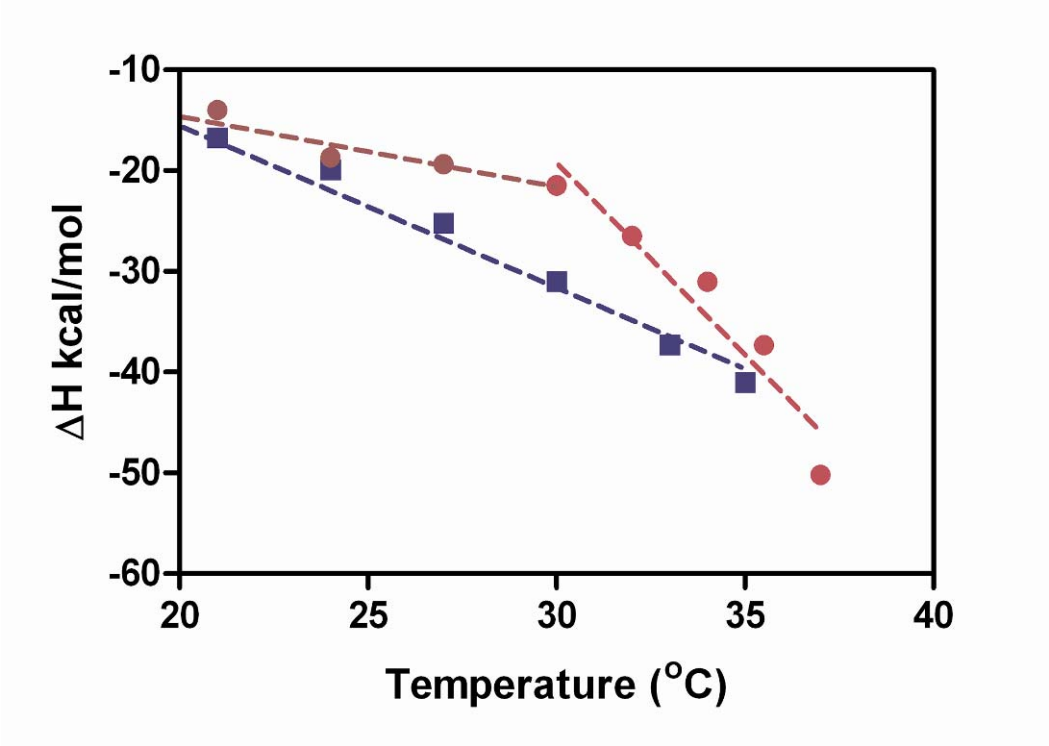

Figure 2. Change in ΔH as a function of temperature for the complexes of APH with neomycin B (blue) and kanamycin A (red). Data are shown with linear regression lines.

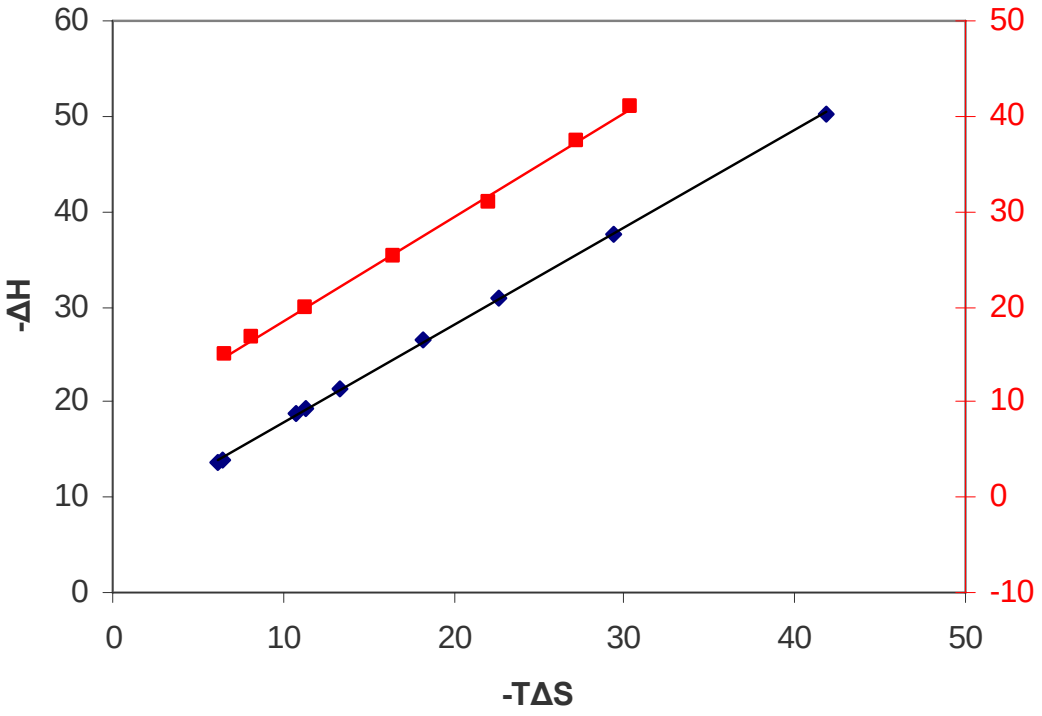

Figure 3. Enthalpy-Entropy Compensation (EEC) plot for kanamycin A (black) and neomycin B (red) complexes with APH. Lines represent linear regression fits.

1.09 and 1.02 for neomycin and kanamycin complexes respectively (R^2= 0.99 in both cases).

Calculation of Accessible Surface Area Change (ΔASA). According to our calculations, formation of kanamycin-APH complex results in burial of 724 $Å^2$ apolar and 1110 $Å^2$ polar surface area. ΔASA values of 806 $Å^2$ and 1030 $Å^2$ were determined for neomycin-APH complex for apolar and polar surfaces respectively. Figure 4 shows ΔASA of amino acids in complexes of APH with kanamycin and neomycin. Significant changes in solvent accessibility were observed in several regions of the enzyme but overall changes seem to be similar in both complexes.

NMR Studies of APH-Aminoglycoside Complexes. Thermodynamic studies yield parameters representing global properties of enzyme–aminoglycoside complexes. In order to understand site-specific implications of these parameters, we used NMR spectroscopy. ^{15}N-^{1}H HSQC (will be referred as HSQC henceforth) spectrum of APH changes dramatically upon binding of aminoglycosides (*22*). HSQC spectrum of neomycin-APH complex (Figure 5A) is shown together with overlaid spectrum of the apoenzyme (Figure 5B) acquired under identical conditions with matched samples. While the apoenzyme spectrum is indicative of a structurally flexible molecule and shows significant resonance overlap, the spectrum of the complex show well-resolved and highly dispersed resonances even for this ~31 kDa protein (264 amino acids). This suggests that APH is floppy in solution and it may even be intrinsically unstructured. Addition of aminoglycosides promotes formation of a well-defined structure. This is also consistent with crystallographic studies of the apo-and-complexed forms of the enzyme where apoenzyme structure is solved with lower resolution and showed high temperature coefficient (*14, 23*).

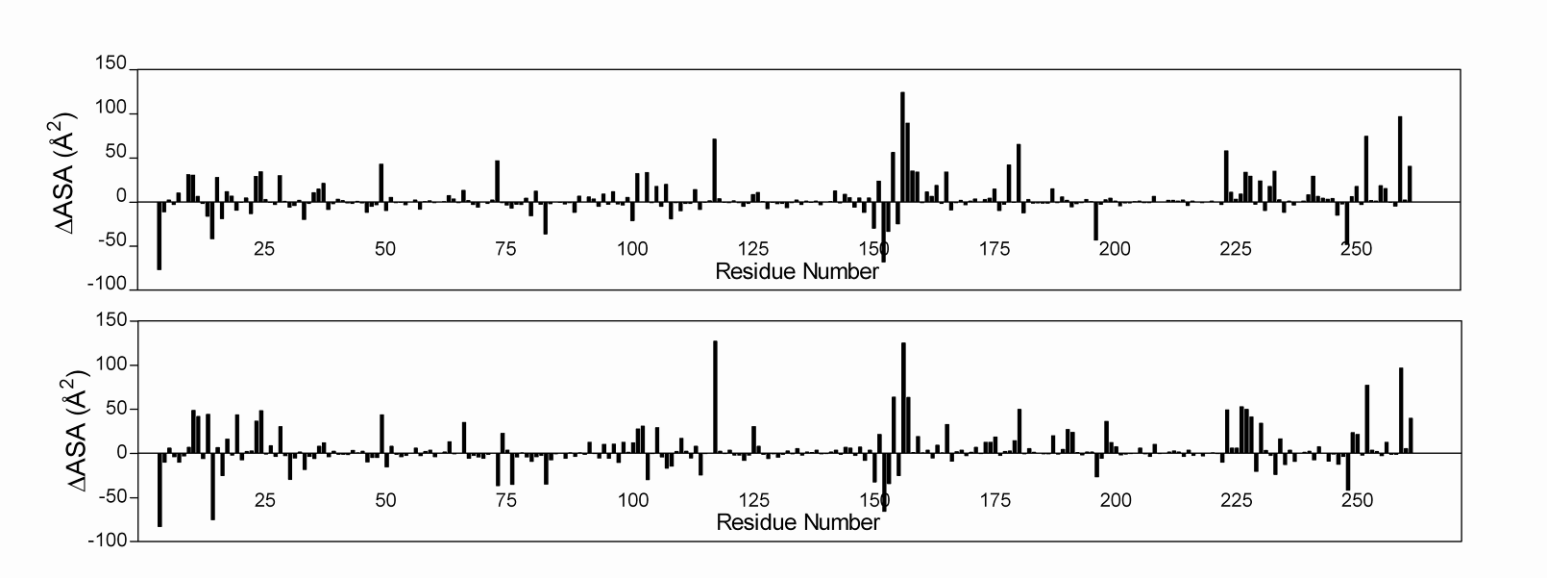

Figure 4. Change of solvent accessible surface area in the formation of kanamycin-APH (top) and neomycin-APH (bottom) complexes.

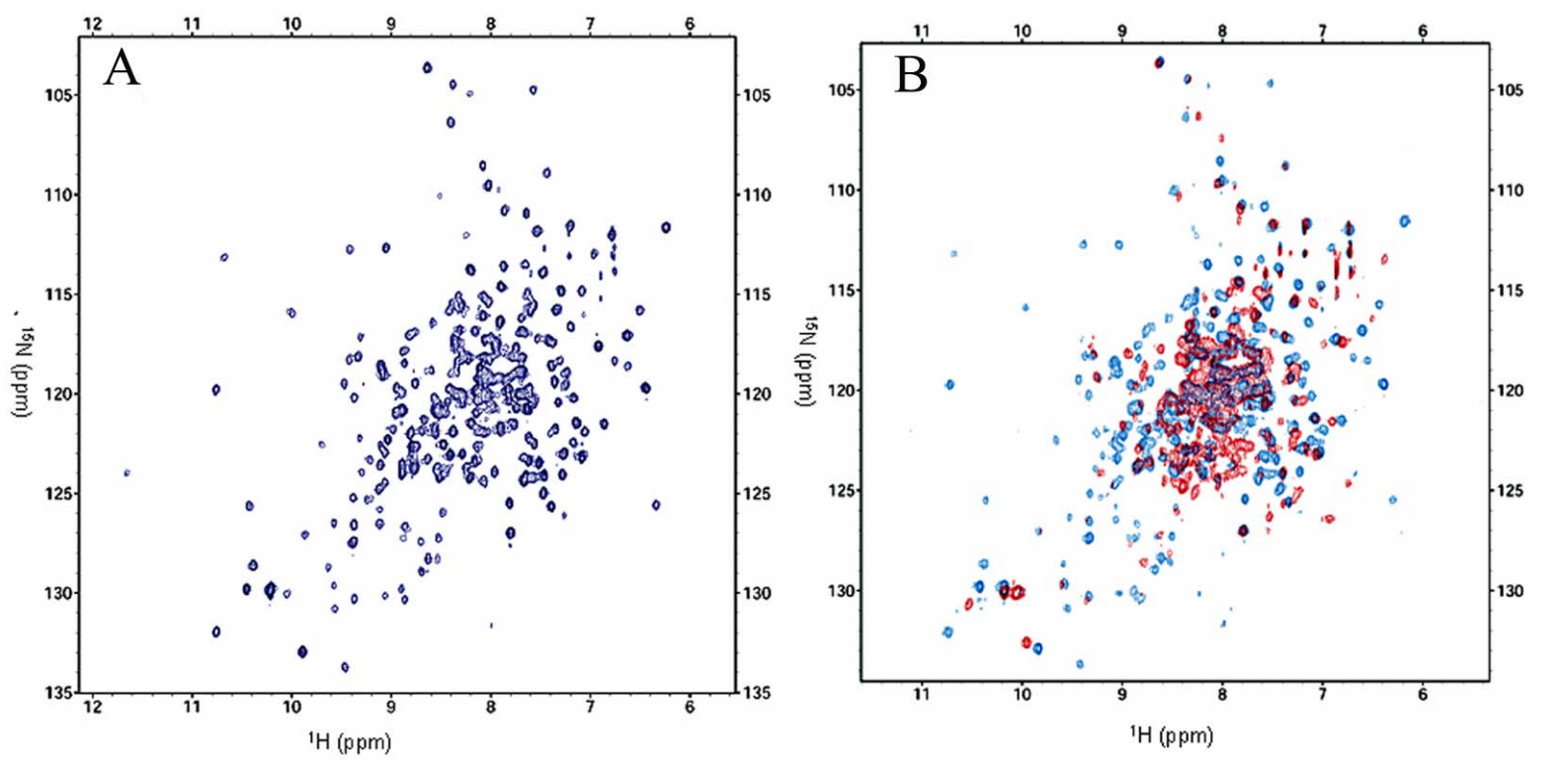

Figure 5. ^{15}N-^{1}H HSQC spectrum of neomycin-APH (A) and neomycin-APH (blue) overlaid with the spectrum of apo APH (red) in (B).

HSQC spectrum of APH with bound kanamycin and neomycin were acquired to determine effect of temperature on the backbone amide resonances of APH between 21ºC and 37ºC. A large number of amides showed temperature-dependent changes in their chemical shifts and more than 40 amides showed different temperature dependence between the two complexes. Figure 6 shows plots of chemical shift versus temperature for selected residues in kanamycin-APH and in neomycin-APH complex.

As illustrated in this figure, some amide protons did not change their chemical shifts as a function of temperature, while some changed in only one of the complexes, and others showed opposite trends. Most notably, ppm versus temperature plots of *four backbone amide protons displayed a break at about 30ºC in the APH–kanamycin complex but not in the neomycin-APH complex*. These amides belong to residues Leu 88, Ser 91, Cys 98, and Leu143 (resonance assignment of APH–aminoglycoside complexes is a work in progress). Expanded region of overlaid HSQC spectra showing Leu 143 peak as a function of temperature in neomycin-APH and in kanamycin-APH complexes is shown in Figure 7. Spectra shown in this figure demonstrates that while the proton chemical shift of Leu 143 is different for kanamycin vs. neomycin complexes at 21ºC, they merge at 31ºC and continue shifting at similar rates after that indicating a break for kanamycin-APH complex at ~30ºC.

Discussion

Solvent Isotopic Effects on Aminoglycoside-APH Complexes. Opposite signs of calculated ΔΔH values of kanamycin and neomycin class complexes (Figure 1) strongly suggests a difference in solvent reorganization during the formation of respective aminoglycoside-APH complexes.

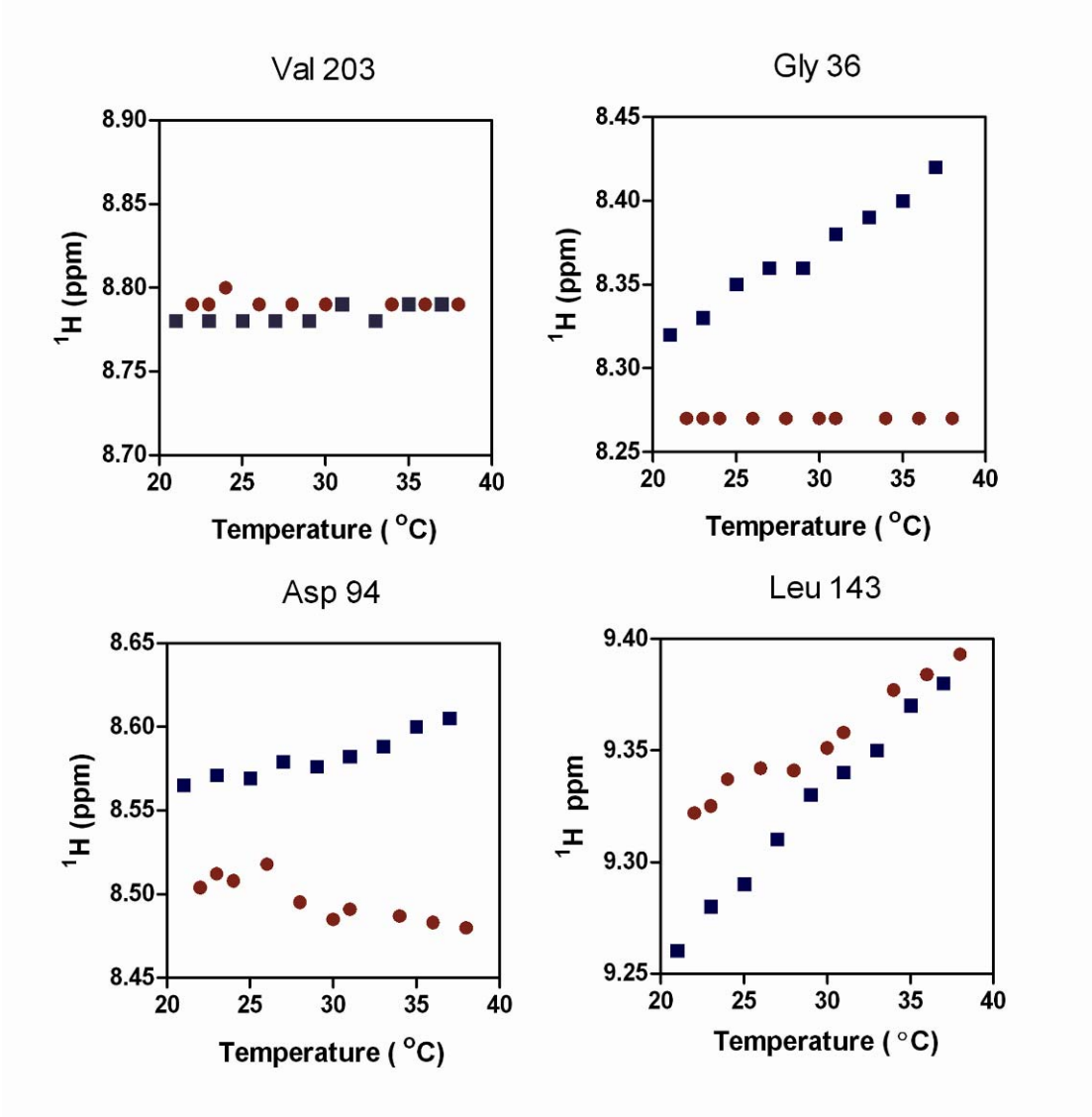

Figure 6. Temperature-dependent changes in the proton chemical shifts of several amino acids of APH in complexes with kanamycin (red) and neomycin (blue).

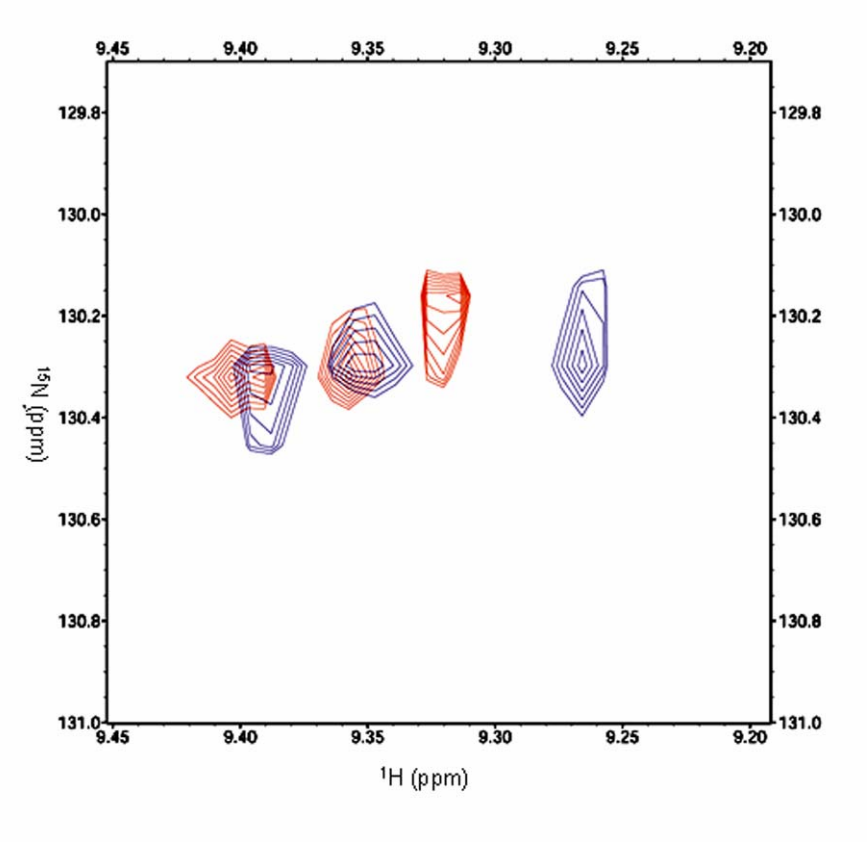

Figure 7. Expanded region of ^{15}N-1H HSQC spectra showing Leu 143 peak as a function of temperature in kanamycin-APH (red, right-to-left 21ºC, 31ºC, and 38ºC respectively) and in neomycin-APH complex (blue, right-to-left 21ºC, 31ºC, and 37ºC respectively).

Critical assumptions of isotopic solvent effect studies must be reminded before we start the discussion of ΔΔH results. These are 1) Complete deuteration of ligand and protein in D_2O experiments, 2) Identical ΔH values associated with proton linkage. Our previous work on APH showed that aminoglycoside-APH binding is linked to protonation/deprotonation of ligand and enzyme ionizable groups (*24*). These functional groups may experience pK_a changes in heavy water which in turn may affect the degree of proton linkage and associated ΔH_{ion} (ionization enthalpy change) in complex formation. Although prediction of such pKa changes in light versus heavy water is not possible, it was shown that changes in protein pK_a values are almost exactly compensated by the difference between hydrogen and deuterium activities (*25*). 3) Structure of ligand, protein and protein-ligand complexes are assumed to be same in H_2O and D_2O. Therefore protein-ligand interactions which include number of hydrogen bonds are considered identical in both solvents.

If these assumptions are met, differential hydration properties of apolar and/or polar groups of ligand and protein are the most likely explanation for the observed ΔH differences in light and heavy water. In the case of kanamycin-APH complex, ΔH is less negative in D_2O, which indicates that heavy water either stabilizes the unbound states or destabilizes the complex. The opposite should be true for neomycin-APH binding.

There are two main structural differences between kanamycin and neomycin class antibiotics (Part I, Figure 1). The first one is the substitution positions of deoxystreptamine ring. Kanamycin class is 4,6-, neomycin class is 4,5-disubstituted. Moreover, ring C is a pentose in neomycins and hexose in kanamycins. Other than these structural differences, relative positions of ring A and C in bound conformations of these

aminoglycosides are very different (*26*). Ring C is closer to ring A in neomycin, allowing formation of intra-molecular hydrogen bonds. These rings are not close in the bound conformation of kanamycin. Difference in the solvent reorganization of kanamycin and neomycin complexes can be explained on the basis of these structural and conformational differences. APH can modify more than ten different aminoglycosides (*15*) and such a flexibility in the organization of water in the binding site may be playing a critical role in its substrate promiscuity.

Aminoglycoside-APH Complexes Show Unusually High Heat Capacity Changes. Heat capacity change (ΔCp) is a thermodynamic parameter closely associated with solvent interactions (*27-29*). ΔCp values reported for various biomolecular interactions are typically negative values, in the range of -0.1 to -0.6 kcal/mol·deg (*30-35*). For carbohydrate-protein interactions, these numbers are usually less than -0.2 kcal/mol·deg (*36*). In comparison, ΔCp values determined for kanamycin-APH (-0.7 and -3.8 kcal/mol·deg) and Neomycin-APH (-1.6 kcal/mol·deg) complexes are unusually high.

Which molecular interaction(s) contribute to ΔCp and why aminoglycoside-APH complexes show such a remarkable change in the heat capacity? Dissection of ΔCp is not an easy task due to the various energetic contributions and temperature dependence of factors such as solvent effects (change in solvation enthalpies) and binding-coupled, temperature dependent molecular processes such as proton linkage and conformational changes. These factors and their relative contributions will be discussed under following subtopics.

Change in the Accessible Surface Area (ΔASA). Apolar and polar contact surfaces (binding interface) of protein and ligand molecules solvated in water molecules in their

unbound states are desolvated and buried upon complex formation. Traditionally, such changes in the accessible surface area (ΔASA) in binding reactions have been considered as the dominant contributor of ΔCp. Contribution of desolvation to ΔCp is proportional to the buried surface area. Loss of apolar surfaces make negative, loss of polar surfaces make positive contributions to the ΔCp. Empirical formulas that have been parameterized from folding and solute transfer data are used in the calculations of ΔASA associated heat capacity changes (*27, 37*). Although there are several reported cases where experimentally determined ΔCp values were found to be matched by computationally calculated ones based on ΔASA, in various other cases consideration of only desolvation was not enough to explain observed ΔCp values (*31, 32, 34, 38, 39*).

According to our calculations, ΔASA for the formation of kanamycin-APH complex is 724 $Å^2$ (apolar) and 1110 $Å^2$ (polar). Values for neomycin-APH binding are 806 $Å^2$ (apolar) and 1030 $Å^2$ (polar). These changes yield 0.037 kcal/mol·deg and 0.095 kcal/mol·deg ΔCp contributions for the kanamycin and neomycin complexes respectively. These results clearly show that ΔASA is not a significant contributor to ΔCp of aminoglycoside-APH complexes.

Proton Linkage and ΔCp of Ionization. Results reported in part II show that binding of aminoglycosides to APH is coupled to protonation/deprotonation of ligand and enzyme ionizable groups. Since ΔH of ionization events (buffer, protein and ligand) also depend on temperature, their contribution to binding ΔCp must be considered. We determined the ΔCp contributions from aminoglycoside amino groups as described by Eftink *et al*. (*40*) which yielded values between -0.12 and -0.14 kcal/mol·deg for the binary neomycin-APH complex. By assuming similar increases in pK_a of amino

functions in kanamycin, one can estimate a contribution of -0.25 to -0.27 kcal/mol·deg for kanamycin-APH complex. Ionization ΔCp of HEPES buffer is 0.012 kcal/mol·deg (*41*). Although these values rule out ΔCp of ionization as a dominant factor, since APH ionazible groups are also a part of proton-coupling, their contributions may be more significant than the buffer and ligand groups.

Conformational Changes. Binding-linked conformational changes such as substantial ordering of a flexible region can have significant negative contributions to the binding heat capacity change (*42*). This is true especially in cases such as unwinding of DNA helix where ΔASA fails to explain the observed ΔCp (*30, 31*). HSQC spectrum of APH indicates highly flexible apo structure becomes a well defined one upon aminoglycoside binding. Significant part of the observed ΔCp may be due to such conformational changes in APH structure. Moreover, our earlier studies with several aminoglycosides showed that at least two conformations of APH-bound aminoglycosides are consistent with the observed NOE distance constraints (*43-46*). These conformations can interconvert to each other at 25ºC and they are different from the conformation of the free aminoglycosides. Thus, binding to enzyme causes conformational changes in ligand as well which should also contribute to the observed large negative values for ΔC_p in both complexes.

We believe that combined effect of all of the factors discussed above results in the highly negative ΔCp of aminoglycoside-APH binding. Although it is not possible to determine quantitative effect of binding-linked conformational changes, it seems to be the dominant factor when the estimated energetic contributions of other factors are considered.

Break in the Heat Capacity Change of Kanamycin-APH Complex. Typically, ΔCp plots represent either linear relations between ΔH and temperature or are non-linear due to the temperature dependence of ΔCp. ΔH of kanamycin-APH binding drastically changes its temperature dependence around 30°C (Figure 2). To our knowledge, there are only few examples of such drastic break points in literature. One of these studies report a very similar ΔCp break at 30ºC for the binding of netropsin to AATT containing hairpin DNA constructs (*47*). By comparing ΔCp profiles and crystal structures of related complexes, Freyer et. al. connected this break to the entrapment of water in the binding interface. Energetic consequence of this solvent structural difference is explained using Dunitz's work (*48*) on isoequilibrium temperature for hydrogen bonding. His study indicates an enthalpy-entropy compensation for hydrogen bonding in water at 27°C. Observation of a break point in ΔCp near water's isoequilibrium temperature strongly suggests a link between these two events.

If the break point in kanamycin-APH plot is also a result of trapped water in binding interface and isoequilibrium temperature of water, this provides additional evidence for the difference of solvent structure in complexes of APH with kanamycin and neomycin. Although ΔASA plots (Figure 4) didn't point to any significant difference in solvent accessibility of residues in aminoglycoside-APH complexes and cannot explain the observed break, NMR studies showed that similar breaks also occurred in the chemical shift changes of several backbone amides as a function of temperature. These residues are in hydrophobic patches distant from active site (Figure 8).

Change of Proton Chemical Shifts as a Function of Temperature. NMR studies of aminoglycoside-APH complexes allowed us to determine specific regions of the enzyme

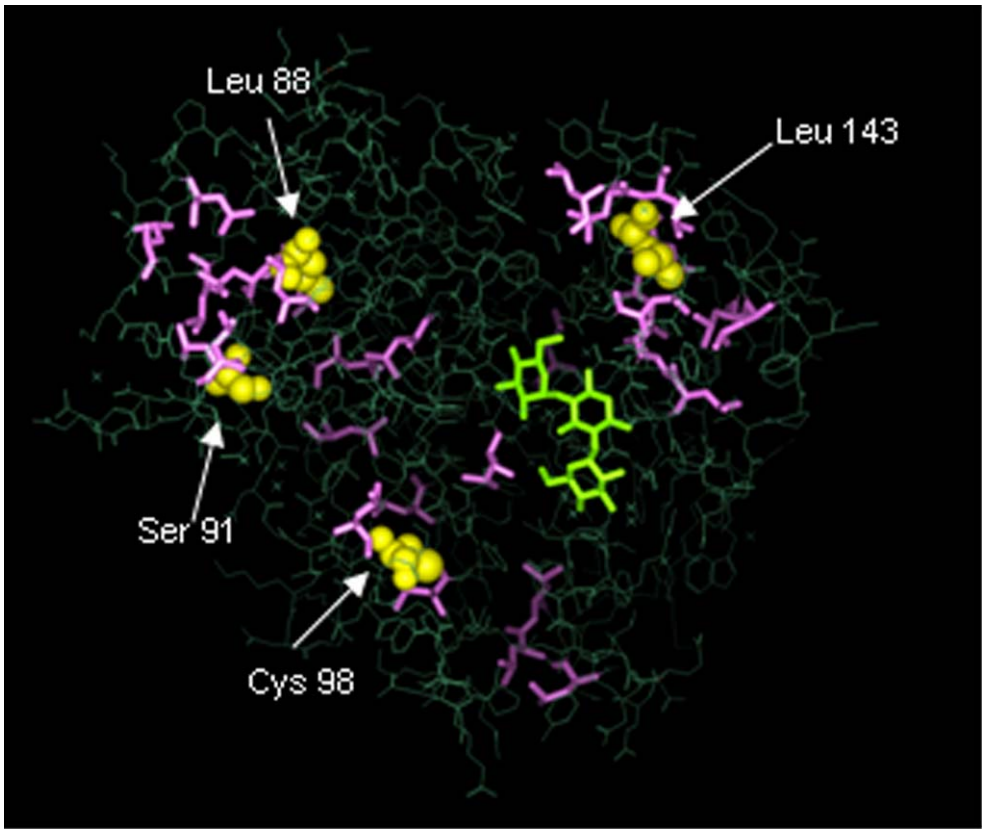

Figure 8. Structure of APH–MgADP–kanamycin complex (*15*). Leu 88, Ser 91, Cys 98, and Leu 143 are shown as cpk model while all leucines are shown in pink. Kanamycin is shown in green.

that may give rise to some of the observed effects in the global thermodynamic properties of these complexes. HSQC experiments yielded unexpected results and showed that >40 backbone amide protons displayed a difference between kanamycin-APH and neomycin-APH complexes in their chemical shifts as a function of temperature. Most importantly, four backbone amides paralleled the difference observed in the ΔC_p values of kanamycin-APH and neomycin-APH complexes. Change in the proton chemical shifts of Leu 88, Ser 91, Cys 98, and Leu 143 showed a break at ~30ºC in the kanamycin-APH complex only. This is likely to represent the effect of altered water structure near these residues, which may have affected hydrogen bonds that these protons are involved in. Even the apparently most buried amino acids, Leu 143 and Cys 98, are flanked by hydrophilic and more exposed amino acids. This would allow formation of hydrogen-bonded water structures around these hydrophobic residues, which are shown in Figure 9. Either a conformational change in the enzyme or even a rearrangement of several side chains above the break point may be sufficient to alter the solvent structure in these regions and affect local hydrogen bond networks. Thus, HSQC experiments may have *highlighted specific solvent reorganization sites of APH*.

An interesting fact is that most backbone amides that show the break at 30ºC are hydrophobic residues and are away from the substrate binding site. Furthermore, they are all distributed the three main hydrophobic patches of the protein, which is probably not coincidental. These results also indicate that reorganization of solvent is not limited to the binding interface or its immediate surroundings when a ligand binds to a macromolecule.

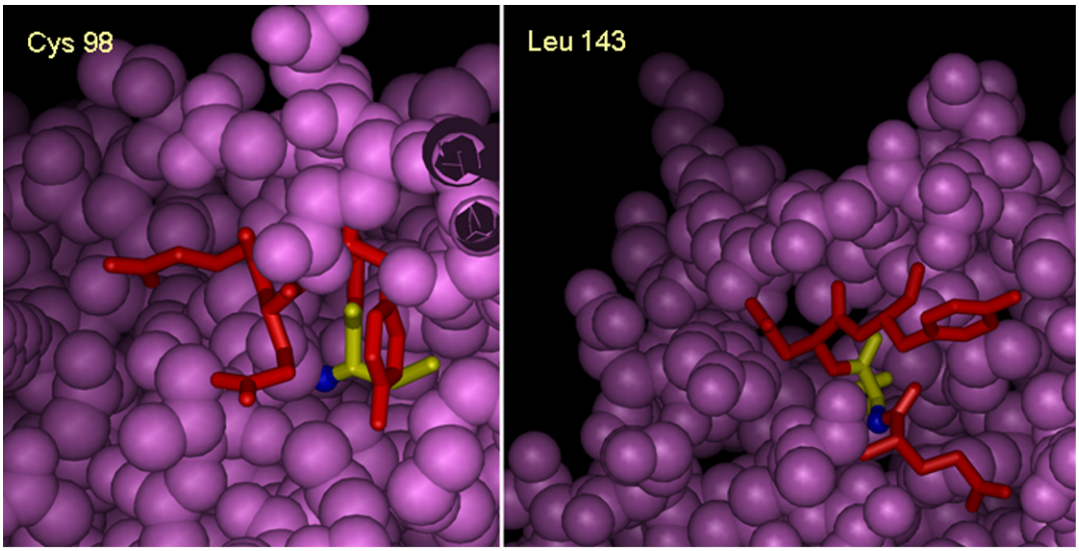

Figure 9. Environment of cys 98 and Leu 143. Left panel: Cys 98 (yellow) and its amide nitrogen (blue) are shown with residues Ser 99, Glu 100, Glu 101, and Tyr 102 (red sticks). Right panel: Leu 143 (yellow with blue nitrogen) is shown with surrounding residues Glu 142, Asp 144, and Tyr 145 (red sticks).

Conclusions

Calorimetric and NMR data presented in this work indicates a difference in solvent reorganization of APH complexes with kanamycin and neomycin class aminoglycosides. Structural and conformational difference between the two drug groups seem to be the reason for different water interactions in respective complexes.

We also observed unusually high heat capacity changes associated with the formation of aminoglycoside-APH complexes. Energetic contributions to binding ΔCp from ΔASA and ionization ΔCp are not significant. We believe that temperature dependence of enthalpy change associated with conformational changes of highly flexible APH and/or aminoglycoside structures may be the dominant ΔCp factor.

Difference in solvent reorganization between the complexes of kanamycins and neomycins were also visible in their change of heat capacity. While both showed heat capacities with large negative values, APH–kanamycin complex revealed a break at 30ºC, above which ΔC_p increased 5-fold.

NMR experiments supported our calorimetric results indicating differences between kanamycin and neomycin complexes. Data showed that, parallel to the break observed in ΔC_p determinations, there was a break in the temperature-dependent change in the chemical shifts of four backbone amide protons in the kanamycin-APH complex. No such break was visible in any amide protons (or nitrogens) in the neomycin-APH complex. We believe, these experiments highlighted specific solvent rearrangement sites away from the substrate binding site in kanamycin-APH complex.

Acknowledgements

I thank Elina Tjioe for ΔASA calculations and Adrianne L. Norris for NMR data collection and analysis.

List of References

References

(1) Baldwin, R. L. (1986) Temperature dependence of the hydrophobic interaction in protein folding. *Proc Natl Acad Sci U S A 83*, 8069-72.

(2) Ben-Naim, A. (1990) Solvent effects on protein association and protein folding. *Biopolymers 29*, 567-96.

(3) Ben-Naim, A., Ting, K. L., and Jernigan, R. L. (1990) Solvent effect on binding thermodynamics of biopolymers. *Biopolymers 29*, 901-19.

(4) Sturtevant, J. M. (1977) Heat-Capacity and Entropy Changes in Processes Involving Proteins. *Proceedings of the National Academy of Sciences of the United States of America 74*, 2236-2240.

(5) Connelly, P. R., Thomson, J. A., Fitzgibbon, M. J., and Bruzzese, F. J. (1993) Probing Hydration Contributions to the Thermodynamics of Ligand-Binding by Proteins - Enthalpy and Heat-Capacity Changes of Tacrolimus and Rapamycin Binding to Fk506 Binding-Protein in D2o and H2o. *Biochemistry 32*, 5583-5590.

(6) Chervenak, M. C., and Toone, E. J. (1994) A Direct Measure of the Contribution of Solvent Reorganization to the Enthalpy of Ligand-Binding. Decreased dH in D2O represents differential interactions with solute and solvent. *Journal of the American Chemical Society 116*, 10533-10539.

(7) Chervenak, M. C., and Toone, E. J. (1994) A Direct Measure of the Contribution of Solvation to the Thermodynamics of Binding. *Biophysical Journal 66*, A359-A359.

(8) Murphy, K. P. (1999) Predicting binding energetics from structure: Looking beyond Delta G degrees. *Medicinal Research Reviews 19*, 333-339.

(9) Spolar, R. S., and Record, M. T. (1994) Coupling of Local Folding to Site-Specific Binding of Proteins to DNA. *Science 263*, 777-784.

(10) Privalov, P. L., Jelesarov, I., Read, C. M., Dragan, A. I., and Crane-Robinson, C. (1999) The energetics of HMG box interactions with DNA: Thermodynamics of the DNA binding of the HMG box from mouse Sox-5. *Journal of Molecular Biology 294*, 997-1013.

(11) Liggins, J. R., and Privalov, P. L. (2000) Energetics of the specific binding interaction of the first three zinc fingers of the transcription factor TFIIIA with its cognate DNA sequence. *Proteins-Structure Function and Genetics*, 50-62.

(12) Myszka, D. G., Sweet, R. W., Hensley, P., Brigham-Burke, M., Kwong, P. D., Hendrickson, W. A., Wyatt, R., Sodroski, J., and Doyle, M. L. (2000) Energetics of the HIV gp120-CD4 binding reaction. *Proceedings of the National Academy of Sciences of the United States of America 97*, 9026-9031.

(13) Hubbard, S. J., and Thornton, J. M. (1993) 'NACCESS' Computer Program, Department of Biochemistry and Molecular Biology, University College, London.

(14) Burk, D. L., Hon, W. C., Leung, A. K. W., and Berghuis, A. M. (2001) Structural analyses of nucleotide binding to an aminoglycoside phosphotransferase. *Biochemistry 40*, 8756-8764.

(15) Fong, D. H., and Berghuis, A. M. (2002) Substrate promiscuity of an aminoglycoside antibiotic resistance enzyme via target mimicry. *EMBO Journal 21*, 2323-2331.

(16) Murphy, K. P. and Freire, E. (1992). Thermodynamics of structural stability and cooperative folding behavior in proteins. *Advan. Protein Chem. 43*, 313-361.
(17) Kay, L. E., Keifer, P., and Saarinen, T. (1992) Pure Absorption Gradient Enhanced Heteronuclear Single Quantum Correlation Spectroscopy with Improved Sensitivity. *Journal of the American Chemical Society 114*, 10663-10665.
(18) Pervushin, K., Riek, R., Wider, G., and Wuthrich, K. (1997) Attenuated T-2 relaxation by mutual cancellation of dipole-dipole coupling and chemical shift anisotropy indicates an avenue to NMR structures of very large biological macromolecules in solution. *Proceedings of the National Academy of Sciences of the United States of America 94*, 12366-12371.
(19) States, D. J., Haberkorn, R. A., and Ruben, D. J. (1982) A Two-Dimensional Nuclear Overhauser Experiment with Pure Absorption Phase in 4 Quadrants. *Journal of Magnetic Resonance 48*, 286-292.
(20) Dam, T. K., and Brewer, F. C. (2002) Thermodynamic studies of lectin-carbohydrate interactions by isothermal titration calorimetry. *Chemical Reviews 102*, 387-429.
(21) Chervenak, M. C., and Toone, E. J. (1995) Calorimetric Analysis of the Binding of Lectins with Overlapping Carbohydrate-Binding Ligand Specificities (Vol 34, Pg 5685, 1995). *Biochemistry 34*, 7966-7966.
(22) Welch, K. T., Virga, K. G., Whittemore, N. A., Ozen, C., Wright, E., Brown, C. L., Lee, R. E., and Serpersu, E. H. (2005) Discovery of non-carbohydrate inhibitors of aminoglycoside-modifying enzymes. *Bioorganic & Medicinal Chemistry 13*, 6252-6263.
(23) Liu, M., Haddad, J., Azucena, E., Kotra, L. P., Kirzhner, M., and Mobashery, S. (2000) Tethered bisubstrate derivatives as probes for mechanism and as inhibitors of aminoglycoside 3'-phosphotransferases. *J Org Chem 65*, 7422-31.
(24) Ozen, C., Malek, J. M., and Serpersu, E. H. (2006) Dissection of aminoglycoside-enzyme interactions: A calorimetric and NMR study of neomycin B binding to the aminoglycoside phosphotransferase(3 ')-IIIa. *Journal of the American Chemical Society 128*, 15248-15254.
(25) Bundi, A. and Wuthrich, K. (1979) Use of amide ^{1}H-NMR titration shifts for studies of polypeptide conformation. *Biopolymers*, *18*, 299-311.
(26) Cox, J. R., McKay, G. A., Wright, G. D., and Serpersu, E. H. (1996) Arrangement of substrates at the active site of an aminoglycoside antibiotic 3'-phosphotransferase as determined by NMR. *Journal of the American Chemical Society 118*, 1295-1301.
(27) Spolar, R. S., Livingstone, J. R., and Record, M. T. (1992) Use of Liquid-Hydrocarbon and Amide Transfer Data to Estimate Contributions to Thermodynamic Functions of Protein Folding from the Removal of Nonpolar and Polar Surface from Water. *Biochemistry 31*, 3947-3955.
(28) Gomez, J., Hilser, V. J., Xie, D., and Freire, E. (1995) The Heat-Capacity of Proteins. *Proteins-Structure Function and Genetics 22*, 404-412.
(29) Habermann, S. M., and Murphy, K. P. (1996) Energetics of hydrogen bonding in proteins: A model compound study. *Protein Science 5*, 1229-1239.

(30) Petri, V., Hsieh, M., and Brenowitz, M. (1995) Thermodynamic and Kinetic Characterization of the Binding of the Tata-Binding Protein to the Adenovirus E4 Promoter. *Biochemistry 34*, 9977-9984.
(31) Datta, K., Wowor, A. J., Richard, A. J., and LiCata, V. J. (2006) Temperature dependence and thermodynamics of Klenow polymerase binding to primed-template DNA. *Biophysical Journal 90*, 1739-1751.
(32) Izutani, Y., Kanaori, K., Imoto, T., and Oda, M. (2005) Interaction of gymnemic acid with cyclodextrins analyzed by isothermal titration calorimetry, NMR and dynamic light scattering. *Febs Journal 272*, 6154-6160.
(33) Berger, C., Jelesarov, I., and Bosshard, H. R. (1996) Coupled folding and site-specific binding of the GCN4-bZIP transcription factor to the AP-1 and ATF/CREB DNA sites studied by microcalorimetry. *Biochemistry 35*, 14984-14991.
(34) Ladbury, J. E., Wright, J. G., Sturtevant, J. M., and Sigler, P. B. (1994) A Thermodynamic Study of the Trp Repressor-Operator Interaction. *Journal of Molecular Biology 238*, 669-681.
(35) Fisher, F. (2001) in *Nature Encyclopedia of Life Sciences*.
(36) Burkhalter, N. F., Dimick, S. M., and Toone, E. J. (2000) Protein-Carbohydrate interaction: Fundamental considerations, in *Carbohydtrates in Chemistry and Biology* (B. Ernst, G. W. H., and P. Sinay, Ed.) pp 863-914, Wiley-VCH, New York.
(37) Gomez, J., and Freire, E. (1995) Thermodynamic Mapping of the Inhibitor Site of the Aspartic Protease Endothiapepsin. *Journal of Molecular Biology 252*, 337-350.
(38) Murphy, K. P., Bhakuni, V., Xie, D., and Freire, E. (1992) Molecular-Basis of Cooperativity in Protein Folding .3. Structural Identification of Cooperative Folding Units and Folding Intermediates. *Journal of Molecular Biology 227*, 293-306.
(39) Guinto, E. R., and DiCera, E. (1996) Large heat capacity change in a protein-monovalent cation interaction. *Biochemistry 35*, 8800-8804.
(40) Eftink, M. R., Anusiem, A. C., and Biltonen, R. L. (1983) Enthalpy Entropy Compensation and Heat-Capacity Changes for Protein Ligand Interactions - General Thermodynamic Models and Data for the Binding of Nucleotides to Ribonuclease-A. *Biochemistry 22*, 3884-3896.
(41) Fukada, H., and Takahashi, K. (1998) Enthalpy and heat capacity changes for the proton dissociation of various buffer components in 0.1 M potassium chloride. *Proteins-Structure Function and Genetics 33*, 159-166.
(42) Vicens, Q., and Westhof, E. (2002) Crystal structure of a complex between the aminoglycoside tobramycin and an oligonucleotide containing the ribosomal decoding a site. *Chemistry & Biology 9*, 747-755.
(43) Serpersu, E. H., Cox, J. R., DiGiammarino, E. L., Mohler, M. L., Ekman, D. R., Akal-Strader, A., and Owston, M. (2000) Conformations of antibiotics in active sites of aminoglycoside- detoxifyiing enzymes. *Cell Biochemistry and Biophysics 33*, 309-321.
(44) Cox, J. R., and Serpersu, E. H. (1997) Biologically important conformations of

aminoglycoside antibiotics bound to an aminoglycoside 3'-phosphotransferase as determined by transferred nuclear Overhauser effect spectroscopy. *Biochemistry 36*, 2353-2359.

(45) Cox, J. R., Ekman, D. R., DiGiammarino, E. L., Akal-Strader, A., and Serpersu, E. H. (2000) Aminoglycoside antibiotics bound to aminoglycoside-detoxifying enzymes and RNA adopt similar conformations. *Cell Biochemistry and Biophysics 33*, 297-308.

(46) Mohler, M. L., Cox, J. R., and Serpersu, E. H. (1998) Aminoglycoside phosphotransferase(3')-IIIa (APH (3')-IIIa)-bound conformation of the aminoglycoside lividomycin A characterized by NMR. *Carbohydrate Letters 3*, 17-24.

(47) Freyer, M. W., Buscaglia, R., Hollingsworth, A., Ramos, J., Blynn, M., Pratt, R., Wilson, W. D., and Lewis, E. A. (2007) Break in the heat capacity change at 303 K for complex binding of netropsin to AATT containing hairpin DNA constructs. *Biophysical Journal 92*, 2516-2522.

(48) Dunitz, J. D. (1995) Win Some, Lose Some - Enthalpy-Entropy Compensation in Weak Intermolecular Interactions. *Chemistry & Biology 2*, 709-712.

PART V. CONCLUSION

In this study, we characterized the global thermodynamic properties of aminoglycoside- APH complexes and dissected some of the determined parameters to gain insight into the structural basis of binding energy. Some of the critical findings and important points that need to be stressed are:

- Calorimetry-derived thermodynamic data reflect global features of the system under study, which includes solvent, protein and ligand molecules in our case. Extreme care must be used in data interpretation and global nature of the observed heat signal and calculated binding parameters, which are a complex combination of several factors sometimes masking each other, must be always kept in mind.
- Aminoglycoside-APH interactions are not dominated by a single type of intermolecular force. Combination of all interatomic forces (hydrogen bonding, Van der Waals forces and ionic interactions) contributes to the binding. Polar and apolar groups of the enzyme and its aminoglycoside substrates as well as the solvent have significant energetic contributions to the complex formation.
- Formation of aminoglycoside–APH complexes are enthalpically-driven and entropically disfavored. Binding is linked to proton transfer which is a consequence of pK_a changes of not only aminoglycoside but also enzyme ionizable groups, possibly remote from the active site.
- Comparative analysis of binding parameters of structurally related aminoglycosides indicate that both 2′- and 6′- positions make enzyme contacts.

  There is no correlation between thermodynamic parameters and size, substitution type or kinetic parameters.

- There are differences in the solvent reorganization of APH complexes with kanamycin and neomycin class antibiotics.
- Complex formation is associated with unusually high heat capacity change (ΔCp) which cannot be explained by accessible surface area change. Drastic conformational changes in the enzyme and substrate structures are believed to make significant energetic contributions to the observed ΔCp term.
- Kanamycin-APH complex shows a break in ΔCp around 30°C. NMR experiments indicate a similar break in proton chemical shifts of four backbone amides which may indicate to specific solvent rearrangement sites.

As future work, priority is on the assignment of APH residues which is an ongoing NMR project in our laboratory to be completed soon. Results of this work will allow us to follow changes in protein structure, as complexes of the enzyme are formed or in response to changing physical parameters, on residue basis.

Osmotic stress experiments to complement isotopic solvent effect studies can also provide additional hints on the solvent reorganization in aminoglycoside-APH binding. Our initial results indicated specific enzyme interactions with the selected osmotic stress agents but we are planning to repeat these calorimetric experiments with other sets of agents which will have minimal or no interaction with APH.

Appendix

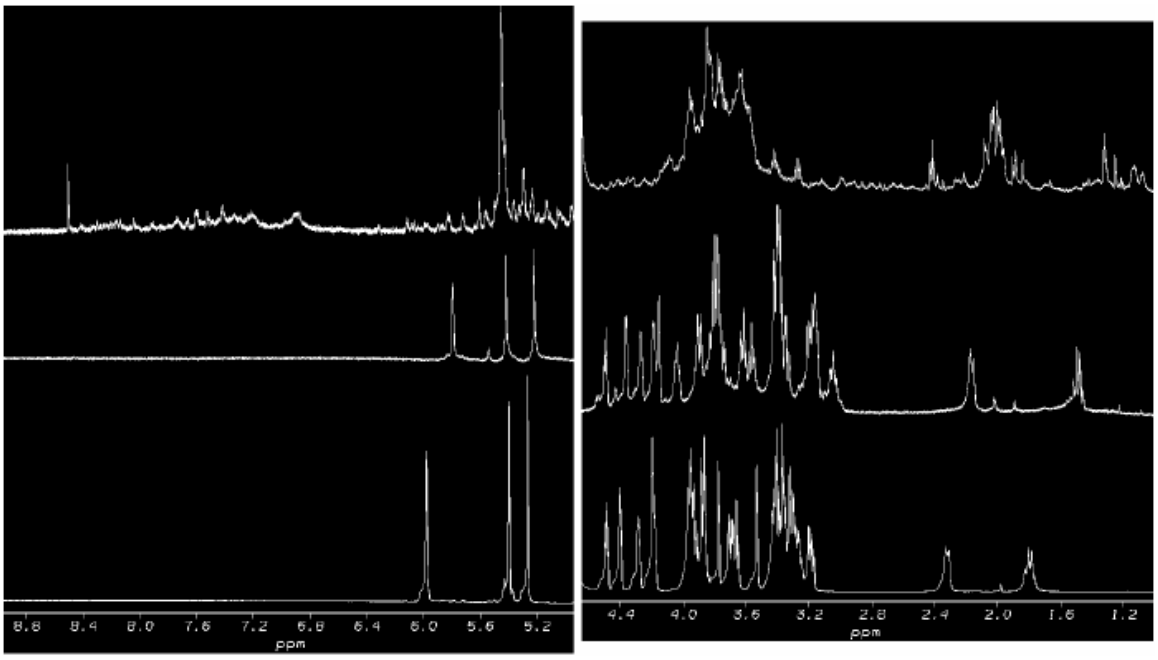

Figure A. ^{1}H NMR spectrum of cell culture medium after harvest (top), purified ^{15}N neomycin (middle), and commercial neomycin (bottom). Note that chemical shifts of aminoglycosides are pH dependent and differences between the commercial and purified neomycin reflect differences between the conditions spectra were acquired.

VITA

Can Ozen was born on May 21, 1976 in Ankara, Turkey. He received his Bachelors of Science degree from the Middle East Technical University in Ankara, Turkey. Then he pursued his Doctor of Philosophy degree in the Graduate Program of Genome Science and Technology at the University of Tennessee in Knoxville.